

General Disclaimer

One or more of the Following Statements may affect this Document

- This document has been reproduced from the best copy furnished by the organizational source. It is being released in the interest of making available as much information as possible.
- This document may contain data, which exceeds the sheet parameters. It was furnished in this condition by the organizational source and is the best copy available.
- This document may contain tone-on-tone or color graphs, charts and/or pictures which have been reproduced in black and white.
- This document is paginated as submitted by the original source.
- Portions of this document are not fully legible due to the historical nature of some of the material. However, it is the best reproduction available from the original submission.

DOCUMENT TITLE

205-6 FINAL REPORT

EXPERIMENT TITLE

Ice Forming Experiment

✓ CONTRACT NUMBER

NAS-8-33150

DOCUMENT DATE

July 30, 1982

PREPARED BY

Department of Atmospheric Science
P.O. Box 3038, University Station
University of Wyoming
Laramie, Wyoming 82071

phone (307) 766-3245

✓ PRINCIPAL INVESTIGATOR

Gabor Vali

KEY PERSONNEL

David C. Rogers
Glenr L. Gordon
John M. White
Terry L. Deshler

SUBMITTED TO

National Aeronautics and Space
Administration
George Marshall Space Flight Center
Marshall Space Flight Center,
Alabama 35812

(NASA-CR-170623) ICE FORMING EXPERIMENT
Final Report, 1976 - 1981 (Wyoming Univ.)
74 p HC A04/MF A01

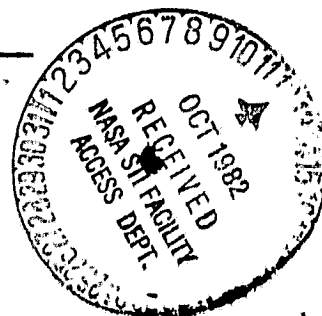
CSCD 04B

N82-33948

Unclas

G3/47 35450

Robert E Smith
ESB



CONTENTS

	page
I. INTRODUCTION AND OVERVIEW	1
II. THE EFFECT OF CLOUD DROPLETS ON THE GROWTH RATE OF ICE CRYSTALS BY DIFFUSION	2
A. Experiments in the Expansion Chamber (EC)	2
B. Qualitative Analog Experiments	8
C. Experiments in the Static Diffusion Ice Chamber (SDI)	12
D. Dimensions of the SDI Chamber	17
III. NUCLEATION OF ICE CRYSTALS IN WINTER OROGRAPHIC CLOUDS	20
A. Measurements of Ice Nuclei with a Continuous Flow Diffusion Chamber	20
B. Submicron Contact Ice Nuclei	22
IV. PUBLICATIONS AND PAPERS	26
V. REFERENCES	27
APPENDIX	29

I. INTRODUCTION AND OVERVIEW

This contract began in 1976 and terminated in 1981. The research effort evolved as NASA's Atmospheric Cloud Physics Laboratory (ACPL) program changed during the contract period and included several contract revisions and no-cost extensions.

Initial involvement of the Department of Atmospheric Science, University of Wyoming, in the ACPL program concerned the design of a low-gravity experiment to assess the effect of the presence of supercooled cloud droplets on the diffusional growth rate of ice crystals. The theoretical work and the feasibility studies conducted on this topic are summarized in section II and culminated in the appended reports and contract documents:

- Status Report No. 1
- 205-2 Experiment Requirements Document
- 205-3 Experiment Specification
- 205-9 Special Hardware Specification Ice Germ Generator.

Later research effort focussed on studying the nucleation of ice crystals in supercooled clouds. Results obtained on this topic are briefly summarized in section III.

The list of publications and papers supported partly or wholly by this contract is given in section IV. Additional papers are planned; their preparation is being supported by other funding.

II. THE EFFECT OF CLOUD DROPLETS ON THE GROWTH RATE OF ICE CRYSTALS BY DIFFUSION

Marshall and Langleben (1954) offered a theoretical paper on the diffusion growth rate of ice crystals in which one of the factors included was the enhancement due to the presence of cloud droplets. They estimated that crystals could grow as much as 10% faster in the presence of droplets, and that the effect can be nearly as important as the ventilation factor.

II.A Experiments in the Expansion Chamber (EC)

Our initial work concentrated on calculating the ice crystal growth rate at different temperatures under the influences of either ventilation or of a proximate liquid water cloud. Such calculations were necessary for optimizing experimental conditions, for assessing experiment sensitivities, and for determining what quantities were to be observed.

In the case of diffusion only, the ice crystal growth equation can be generally written (e.g., Marshall and Langleben, 1954 or Mason, 1971):

$$dm/dt = S_i/f(T,P) \quad (1)$$

where m is crystal mass, t is time, S_i is the supersaturation of the environment with respect to ice and $f(T,P)$ is a slowly varying thermodynamic function which depends on the temperature and total pressure. The effects of ventilation or of a water cloud are usually included through multiplying factors. For ventilation, the factor is $(1+0.23\sqrt{Re})$ where Re is the Reynolds number of the airflow around the crystal, and for a water cloud, the factor is $(1+kr)$ where k is a measure of the water content (sum of the cloud drop radii per unit volume), and r is crystal radius (Marshall and Langleben, 1954). This equation (1) was transformed from dm/dt to dD/dt where D is crystal diameter (an easy quantity to measure experimentally), and growth rates were calculated for the range of typical atmospheric conditions. The results are plotted in Figures 1a and 1b in terms of the percent change of either the ventilated or water cloud cases compared with diffusior growth only. Several important experimental aspects can be deduced from this figure:

1. The effect for the water cloud is most significant for large water contents and large ice crystals.
2. The effect of ventilation is comparable in magnitude to that of the water cloud; therefore, for the ice forming experiments, careful attention must be paid to

ORIGINAL PAGE IS
OF POOR QUALITY

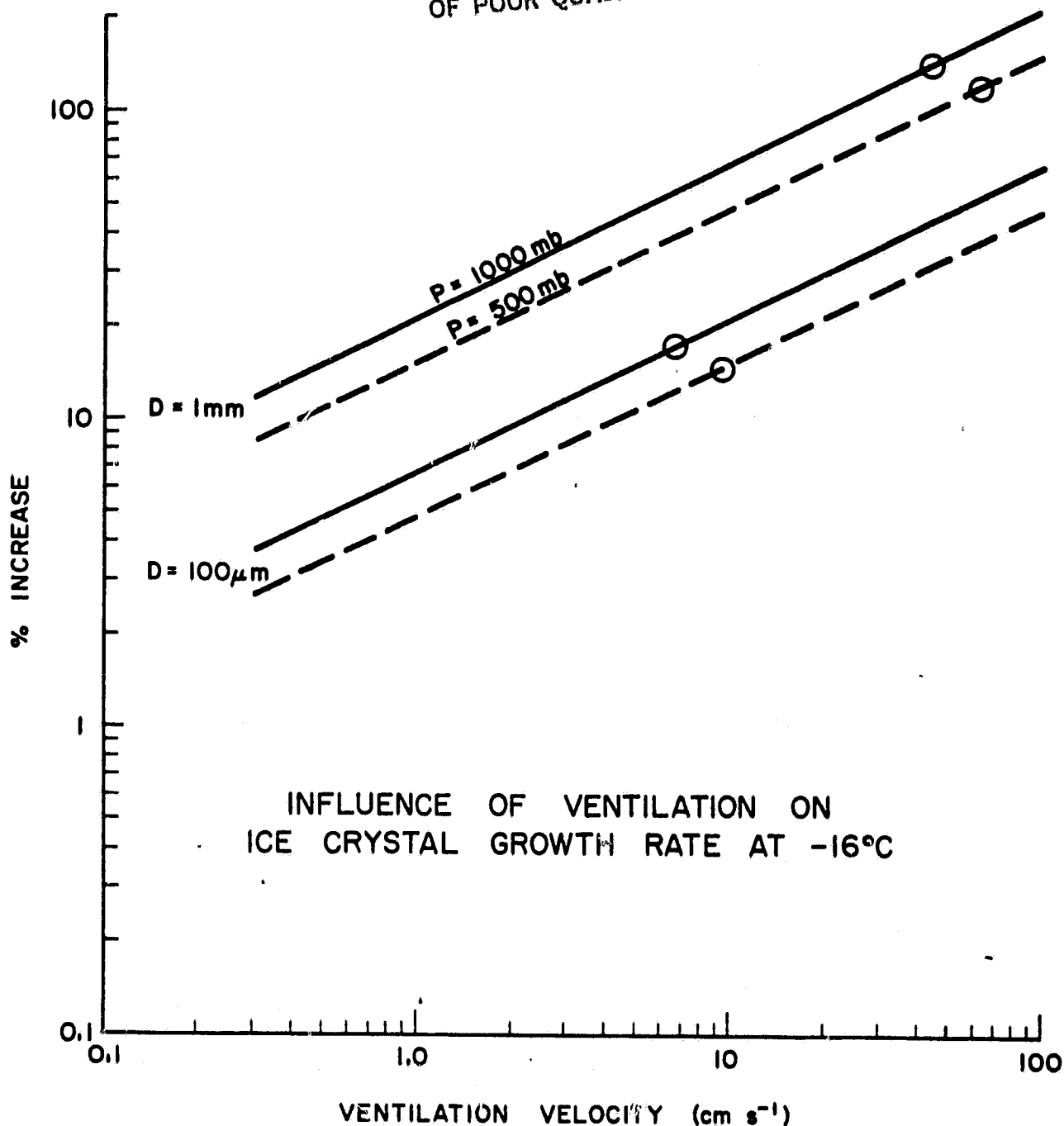


Figure 1a. Influence of ventilation on the growth rates of ice crystal diameters at -16°C . The increase in growth rate is shown as a percent increase over the growth rate by diffusion only. The effect is shown as a function of ventilation velocity for two diameters (D) of crystals and for two different ambient pressures (P); circles show estimated terminal velocities of hexagonal plate type crystals falling freely in air. Calculations are based on the theory of Marshall and Langbein (1954).

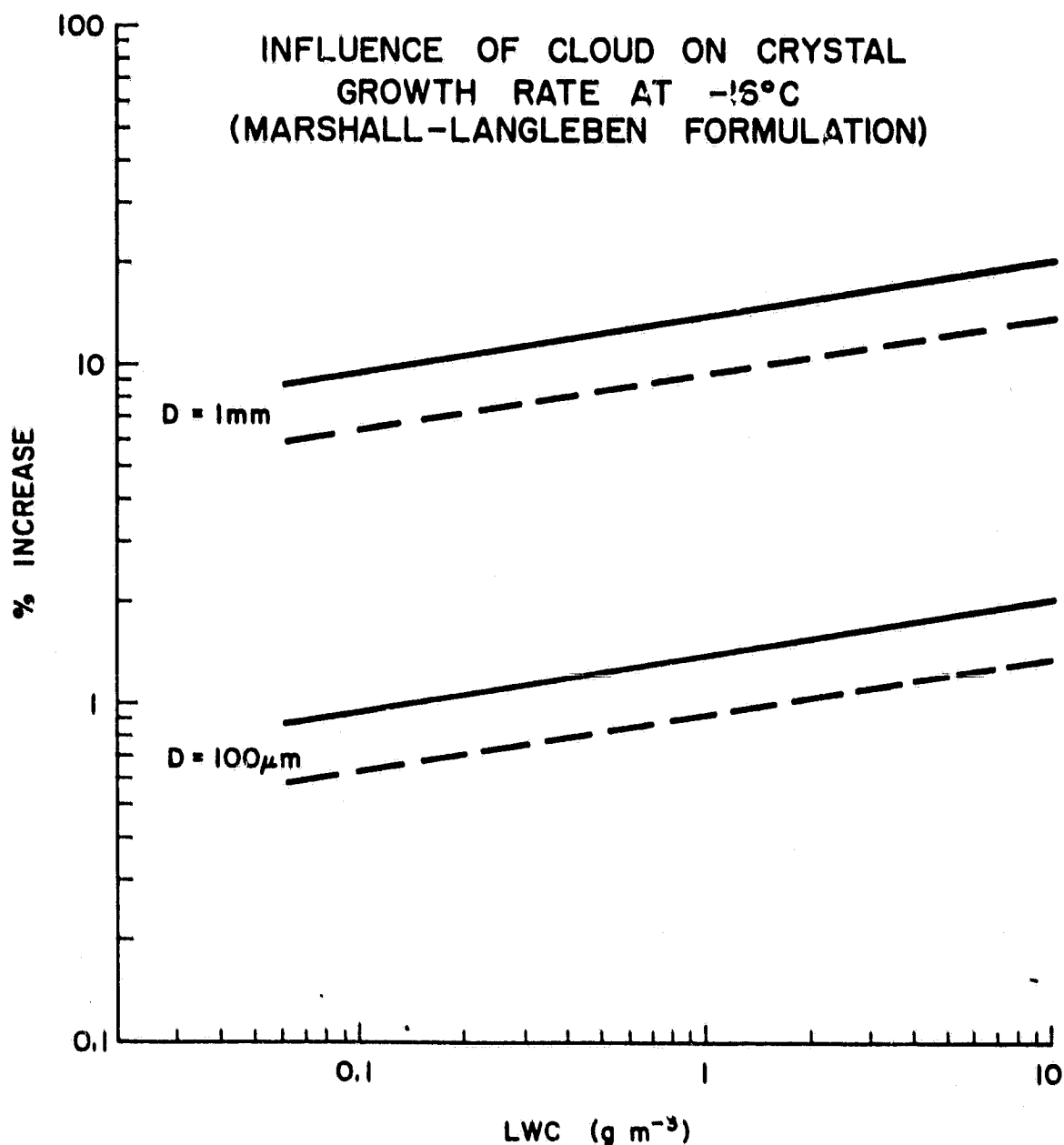


Figure 1b. Influence of the presence of a liquid water cloud on the growth rates of ice crystal diameters at -16°C . The increase in growth rate is shown as a percent increase over the growth rate by diffusion only. The effect is shown as a function of cloud liquid water content for two diameters (D) of crystals and for two different values of cloud droplet concentration (n). Calculations are based on the theory of Marshall and Langleben (1954).

the stilling of air motions in the ACPL chambers.

3. The increase in growth rate for the water cloud case is about 10% over the diffusion-only case. Thus direct measurement of the effect is difficult. To measure a 10% effect to an accuracy of $\pm 10\%$ over time intervals of the order of 100 seconds, for a typical crystal growth rate of $1 \mu\text{m/s}$, would require optical resolution by the photographic system of better than $1 \mu\text{m}$ in the sensitive experimental volume (SEV), i.e., $\pm 10\% \times 10\% \times 100\text{sec} \times 1 \mu\text{m/sec} = \pm 1 \mu\text{m}$. Thus, while the crystal growth rate is of fundamental interest, its accurate measurement may not be directly attainable, and some additional measure of the effect of the water cloud is desirable.

As the crystal grows, the environmental humidity around the crystal will fall to a value between water and ice saturation, and the water drops in this region will evaporate (the Bergeron-Findeisen phenomenon). Thus a droplet-free zone (DFZ) of roughly spherical shape will form around the crystal and will expand with time as the crystal grows. The boundary of this zone and its expansion with time correspond with the growth rate of the crystal, and it offers a better characteristic to measure experimentally. Some calculations were performed to ascertain the rate of movement of the DFZ. These calculations are presented in Figure 2 for two different approximate approaches. The first approach (mass balance) equates the mass flux to the crystal (based on the theoretical growth rate for an environment maintained at water saturation at infinite distance) to the mass flux out of a concentric spherical annular volume containing cloud droplets; i.e., it is assumed that all of the vapor comes from the evaporating cloud droplets. The second approach (labelled M-L) uses the results of Marshall and Langleben (1954): they calculated the steady-state profile of humidity versus radial distance from the crystal for different water contents of the cloud. Then, given this steady-state environment, the droplet growth (or evaporation) equation was used to predict how long it would take to evaporate a droplet of given size located at a specified radial distance. The actual rate of propagation of the DFZ is expected to lie somewhere in the vicinity of these two approximations. It is seen that experimental times of the order 50 to 100 seconds should produce a DFZ of the order 0.5cm in radius and that the rate of propagation is fairly rapid (about $5 \mu\text{m}$ per second). Thus, an experimental measurement of the DFZ would require more modest instrumental capabilities, compatible with the proposed ACPL photographic system.

A complicating factor to observing the DFZ is the presence of intervening droplets. This problem is illustrated in Figure 3. The DFZ is indicated at several

ORIGINAL PAGE IS
OF POOR QUALITY

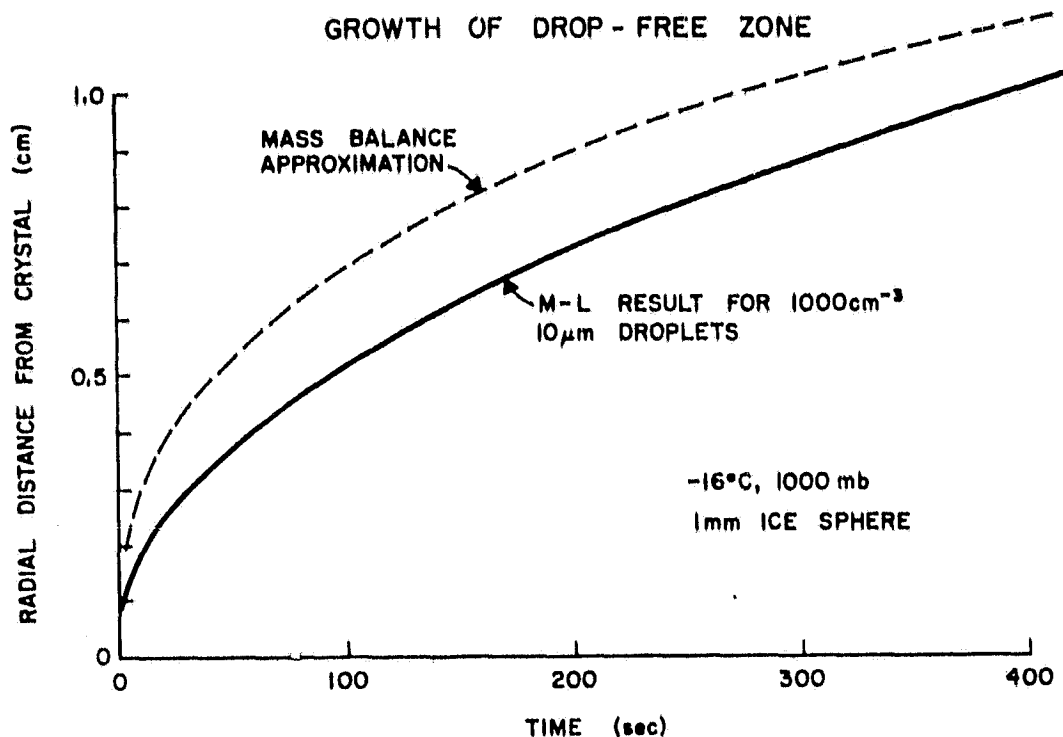


Figure 2. Two estimates of the rate of expansion of a spherical drop free zone around a growing ice crystal. The Mass Balance Approximation equates the vapor flux to the crystal (growing in an environment that is saturated with respect to water at infinite distance) with the vapor flux out of a concentric spherical annular volume containing cloud droplets; i.e., all vapor comes from evaporating cloud droplets. The M-L calculation uses the Marshall and Langbein (1954) equation of the steady state radial profile of relative humidity surrounding a crystal growing in an environment of cloud droplets ($1000/\text{cm}^3$, $10\mu\text{m}$ diameter, liquid water content of $0.52\text{g}/\text{m}^3$); within this environment, the usual droplet growth equation (e.g., Mason, 1971) is used to estimate the time to evaporate the $10\mu\text{m}$ droplets to zero size.

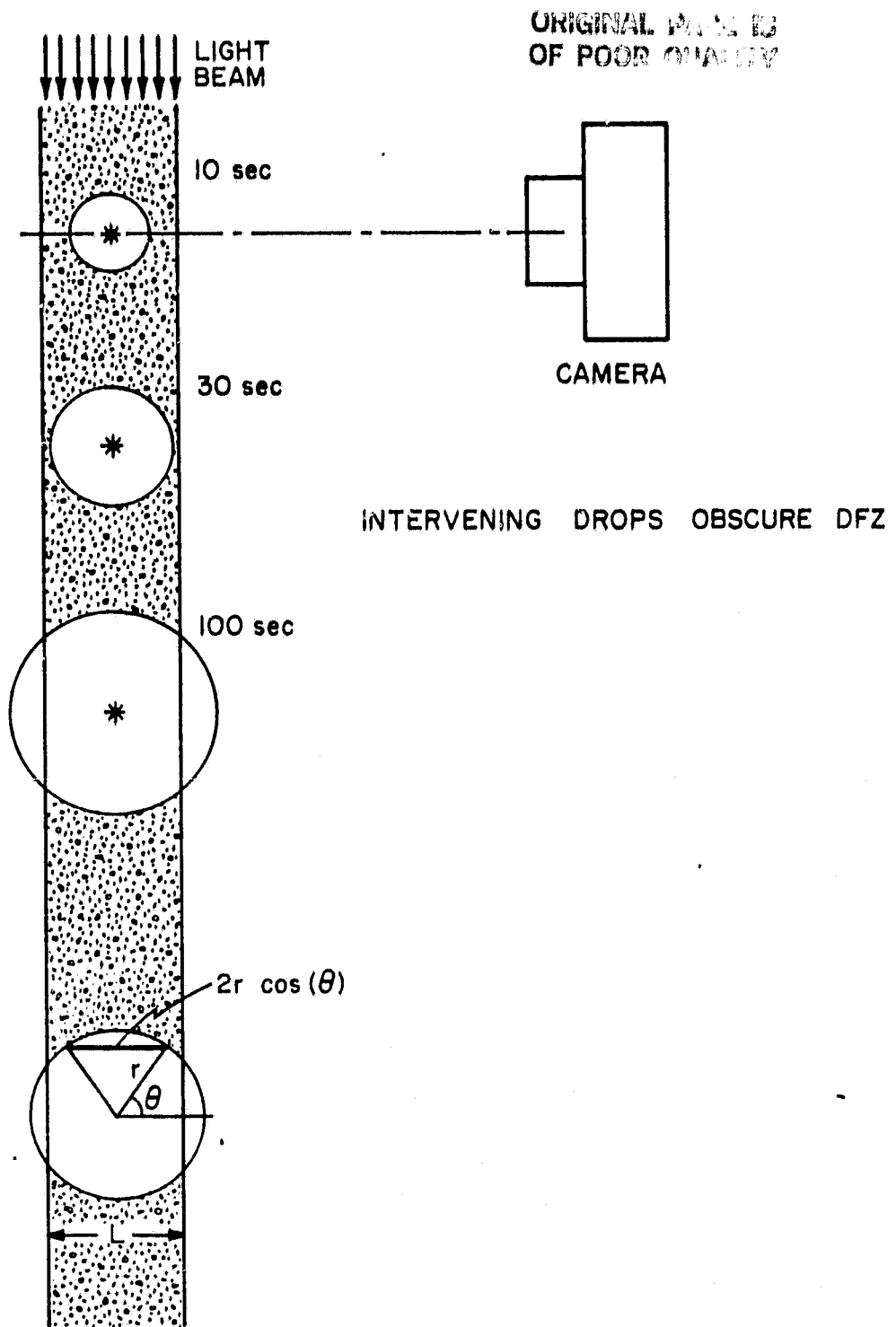


Figure 3. Illustration of the interference of intervening drops in identifying the boundary of the drop free zone (DFZ) which forms around a growing ice crystal. Stippled area shows the illuminated part of the cloud ($L = 0.65\text{cm}$ in ACPL design). Circles show estimated size of DFZ at indicated times after the cloud forms by expansion.

different times; it is initially smaller than the illuminated width and later becomes larger. If the boundary of the DFZ is defined where the droplet concentration falls to 50% of the surrounding value, then this margin will be difficult or impossible to identify for short time periods (10 seconds in the figure). At later time periods, the margin becomes easier to identify as the illuminated width containing cloud droplets becomes a smaller fraction of the DFZ size. This aspect is made quantitative by the geometric analysis in Figure 3. The intervening illuminated droplets occupy a fraction of the total illuminated width given by $(1-2r \cos(\theta)/L)$, where L is the illuminated width (0.65cm in the ACPL design), r is the radial size of the DFZ, and the angle θ is measured from the optical axis of the camera. This fraction was calculated for estimated sizes of the DFZ at different times (using the Marshall-Langleben approximation mentioned earlier and shown in Figure 3) and for an illumination width of 0.65cm. The fraction is plotted as a function of the distance from the crystal center (i.e., size of the DFZ) at different times in Figure 4. The important aspects of this figure are:

1. The DFZ (defined at 50% reduction) is most sharply resolved when the slit is narrow compared with the DFZ (i.e., steeply sloped lines where the fraction is 50%).
2. The DFZ cannot be identified until about 10 seconds have passed; this time would be even larger if a more restrictive definition for the DFZ boundary were used, for example, where the droplet concentration falls to 10% of the surrounding value.
3. Experimental times on the order of 400 seconds are anticipated to obtain a DFZ of about 1cm radius.

The impact of this figure on the experimental design is the suggestion to have either an adjustable slit width or else one which can be selected to suit the particular experimental conditions to optimize identifying the DFZ.

II.B Qualitative Analog Experiments

We had initially proposed to perform the crystal growth experiments by using expansion chamber in the ACPL. A mock-up of the ACPL expansion chamber was constructed (not exactly to scale) in order to assess the ability of the proposed photographic and illumination system to document the DFZ. The chamber was 20cm in diameter and 25cm long (Figure 5). The chamber was kept at room temperature, and the chamber volume was kept at water saturation by a pool of standing water on the bottom of the chamber. An aerosol (room air or the combustion products of a burned match) was introduced into the chamber and mixed uniformly. Next, the chamber was overpressured (100mb over room pressure), and

ORIGINAL PAGE IS
OF POOR QUALITY

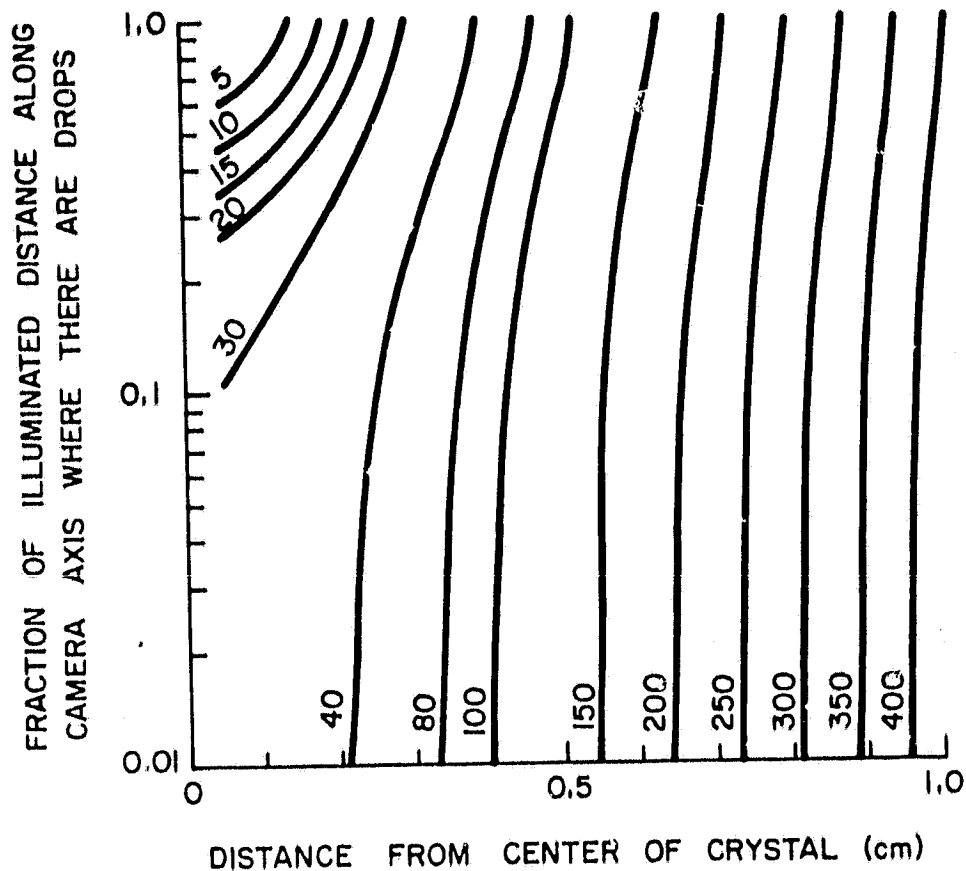


Figure 4. Calculation of the interference of intervening drops in identifying the boundary of the drop free zone (DFZ) at different times after the cloud forms by expansion. The abscissa is the size of the DFZ, estimated by a method using the equations of Marshall and Langleben (1954). Ordinate is fraction of drops in the illuminated width which are outside of the DFZ. If the boundary of the DFZ is defined where the fraction is 0.5, then the uncertainty in locating the boundary from photographs is smallest where the time lines have steep slopes near 0.5.

ORIGINAL PAGE
BLACK AND WHITE PHOTOGRAPH

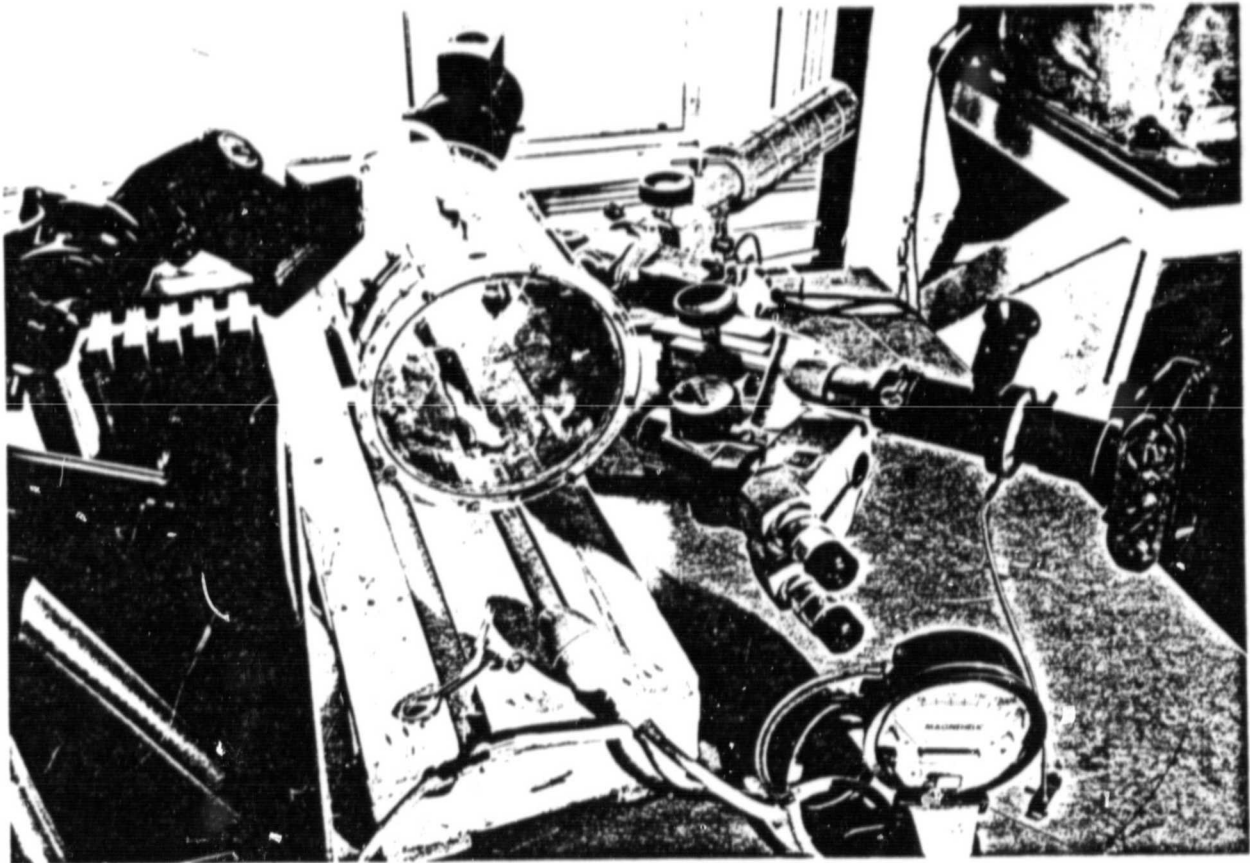


Figure 5. Expansion chamber used for experiments analogous to the ice forming experiment. Visual inspection and photography are through transparent chamber ends; illumination window is on left. Chamber volume is 10 liters.

time was allowed for the chamber to come to thermal and vapor equilibrium and for stilling of air motions to occur (several minutes). A controlled expansion was produced by allowing some of the excess pressure to escape through a small orifice in the piping. The expansion produced adiabatic cooling within the chamber, and in response a cloud formed within a few seconds. Since the interior of the chamber was then colder than the walls, a convective circulation was induced and was evidenced by the motion of the cloud drops after 2 to 5 seconds. Thus, the useful part of this experiment lasts only a few seconds. However, our preliminary calculations and experiments indicated that the DFZ formed quickly enough that a few seconds produced a visually discernable DFZ having dimensions of a few millimeters. In this case, the DFZ was produced by the vapor sink of a small crystal of NaCl (about .4mm dry) which was cemented to a hair and was suspended in the central part of the chamber. NaCl is hygroscopic and soluble, and so the crystal deliquesced into a salt solution droplet. Also, the vapor pressure at the surface of the droplet was less than that of the saturated environment. Thus the solution droplet was continually extracting water vapor from the chamber in analogy with a growing ice crystal. The effect of the salt crystal is not constant, but depends upon several variables which we made little effort to control stringently. For example, the vapor pressure depression depends upon the molality of the solution which in turn depends upon the initial size of the dry crystal, the time that the crystal has spent in the saturated environment, the total pressure and the temperature. Calculating the expected behavior of the salt solution droplet would be a difficult task and probably not worth the trouble since the benefits expected from this simulation were primarily in terms of evaluating the photographic detection system. An estimate of the magnitude of the effect can, however, be easily made. The deliquescence point of NaCl is about 75% relative humidity, and this value will be maintained for as long as there is some crystalline salt present (until the droplet grows to about .75mm diameter). Thereafter, the vapor pressure depression diminishes slowly as the droplet grows further. The analogous case for an ice crystal growing in a water saturated supercooled environment corresponds initially to a temperature of about -30°C , where saturation with respect to ice is 75% of the value with respect to water. At warmer temperatures, the vapor pressure depression of the ice crystal diminishes, becoming approximately 90% at -11°C ; this corresponds then to the salt solution droplet after some growth. In this manner, the salt solution droplet produces an effect which is roughly comparable in size and magnitude with the ice crystal experiment.

ORIGINAL PAGE IS
OF POOR QUALITY

An example photograph of the DFZ produced in this manner is shown in Figure 6. The most significant uncertainties of this experiment are with respect to the induced convective air circulation which limits the experimental time period to a few seconds. An experiment such as this one is an easy and definitive way to test the abilities of the proposed ACPL photographic system to detect the DFZ.

II.C Experiments in the Static Diffusion Ice Chamber (SDI)

In modifications of the original ACPL experimental schedule, it was proposed to construct only the static diffusion chamber for the early flights. Accordingly, we proposed some preliminary qualifying experiments with this chamber in the supercooled range of operation. Four different experiments were suggested, not as substitutes for the expansion chamber experiment, but as preliminary experiments having independent scientific interest, and which could provide information on the operating characteristics and capabilities of the experimental systems. Because of particle sedimentation and buoyant air circulations, a low gravity environment is needed for all four experiments. Timelines for these suggested experiments are elaborated in greater detail in the draft Experiment Specification (DR 205-3).

Procedures for the four ancillary experiments are briefly summarized in this section. Three utilize the SDL in a rapid expansion mode with the chamber initially isothermal at a temperature below 0°C and at ice saturation. The temperature of the air cools rapidly with the controlled rapid expansion. The coldest temperature is determined by the amount and rate of expansion. Following the expansion, the air temperature and vapor fields slowly recover to their initial, pre-expansion values. The recovery period lasts for several thermal and vapor time constants of the chamber, and eventually the initial temperature and vapor fields become reestablished. It was the transient recovery period which was to be studied by the photographic records for three of these experiments. The fourth experiment was to use a temperature difference between the plates of the chamber to form droplets in a supersaturated zone in the chamber; this situation is quasi-steady. For all of these experiments, NaCl aerosol was to be used. It was anticipated that the aerosol should be characterized by the aerosol system for its dry size distribution and by the continuous flow diffusion chamber for its activation spectrum.

ORIGINAL PAGE
BLACK AND WHITE PHOTOGRAPH



Figure 6. Example photograph of drop free zone which forms around NaCl solution drop in the expansion chamber. The dark drop free zone is about 0.7cm diameter.

The four experiments are:

#1 evaporation of droplets to walls

A cloud of supercooled water droplets can be formed by a short, rapid expansion. Calculations by the ACPL Simulator for this experiment are shown in Figures 7a, 7b and 7c and suggest that the droplets will grow within the first 4 seconds to peak sizes of about $5\mu\text{m}$ radius. Thereafter, the interior of the chamber will warm by conduction from the walls, and the initial pre-expansion vapor and temperature fields will become reestablished. This will be exhibited by the evaporation of the liquid water droplets beginning near the walls and progressing toward the center; the cloud is completely gone after about 50 seconds. Although the temperature changes significantly during the period from 4 to 10 seconds, the water cloud in the center region of the chamber is relatively unaffected by the walls for approximately 6 seconds.

The phenomena of interest are the rate of evaporation of the droplets and the ability of the photographic system to document the evaporation. Adjustments of the initial and final conditions can delineate the limits of capabilities of the photographic system and can be used to optimize the definition (sharpness) of the boundary of the drop free zone as it propagates inward. The available adjustments, however, tend to work in opposite directions: on the one hand, increasing the aerosol concentration will enhance the contrast along the edge of the DFZ boundary, but on the other hand, it also reduces the droplet sizes and therefore taxes the sensitivity of the photographic system. For example, estimated maximum drop radii using aerosol concentrations of 100 to $3000/\text{cm}^3$ vary from 6 to $2\mu\text{m}$, respectively. Therefore, in order to better examine the capabilities of the photographic system, additional iterations may be desirable, where the aerosol concentration is varied.

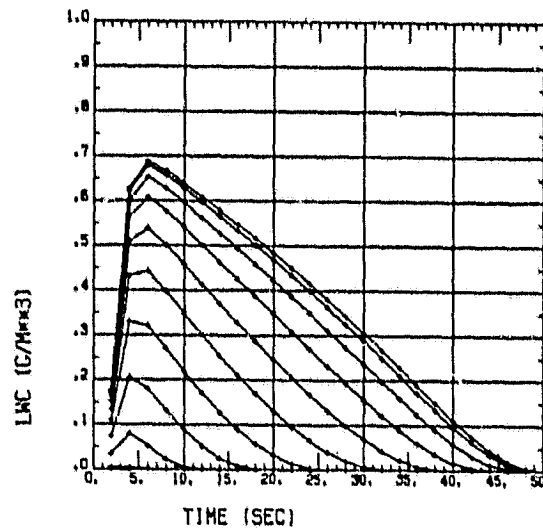
The overall experimental time required for each sequence of expansions at two different initial temperatures (-5°C and -15°C) is about 940 seconds (16 minutes).

#2 ice germ generator and expansion-formed cloud

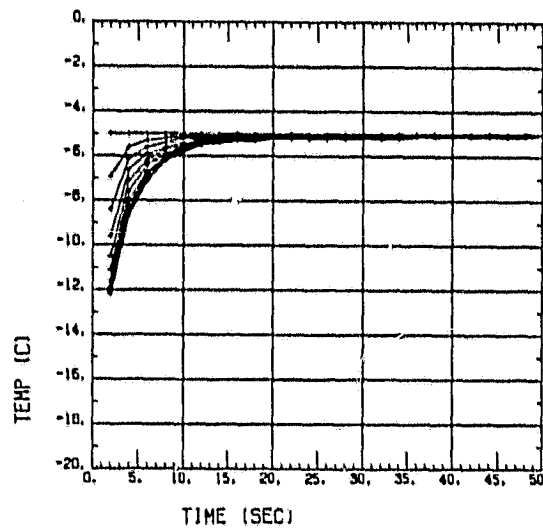
An ice germ generator was designed for insertion into the supercooled chamber through a probe port. The generator produces ice on its tip while the payload specialist controls and observes its operation. Formation of the ice germ is followed by a cloud-producing expansion and photographic recording of the effect of the ice crystal upon the liquid water cloud. Since the effects of the walls

ORIGINAL PAGE IS
OF POOR QUALITY

a)



b)



c)

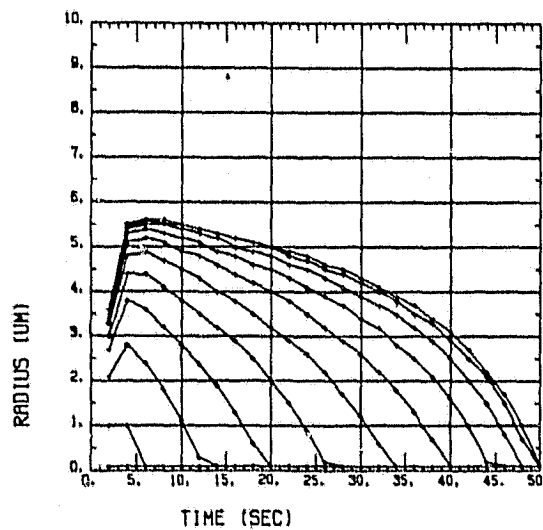


Figure 7a, 7b and 7c. Time traces of temperature, liquid water content and drop radii in the SDI as predicted by the ACPL Simulator. With initial conditions of ice saturation at -5°C , a rapid expansion occurs at time zero (-50mb/s for 2 seconds). Values are shown at ten evenly spaced grid locations from the wall to the center. SDI plate spacing is 3cm; grid spacing is 0.15cm.

dominate all processes in the SDI, the time allowed for observing the droplet evaporation around the crystal is rather limited (as in experiment #1) and is a critical factor for this experiment. Details of the ice germ generator are described in documents 105-9 and 205-9 included in the appendix. Three modes of operation were considered for the ice germ generator: the liquid drop dispenser, the ice ejector and the nucleating substrate fiber. An advantage provided by the low gravity environment is in seeing where an ejected ice particle will go, and if its trajectories are reproducible and controllable for later use in the expansion chamber experiment.

#3 ice germ generator and thermal gradient-formed cloud

In this experiment the generator is inserted into the chamber prior to cooling to a sub-freezing isothermal condition. The generator is used to produce ice on its tip while the payload specialist controls and observes its operation. Next, the chamber wall temperatures are adjusted to produce nominal water supersaturation in the SEV. A water cloud forms in the central region of the chamber except near the ice crystal. The DFZ around the crystal will extend from the crystal surface (at ice saturation) outward to where the saturation level increases to water saturation. Since the vapor flux to the ice crystal is much smaller than the flux from the warm chamber wall, the ice crystal will be a significant vapor sink only over a relatively small region (at least for as long as the crystal remains small). Therefore, the DFZ will be a steady, or quasi-steady, feature. Its dimensions will depend upon the crystal temperature, the nominal central supersaturation, the crystal size and the droplet concentration.

This experiment is more difficult to analyze because of two dimensional temperature and vapor gradients. However, it has distinct advantages for assessing the sensitivity of the DFZ to the various cloud conditions which are not transient. For example, by simultaneously adjusting the warm and cold plate temperatures, the central temperature could be changed while keeping the nominal water supersaturation constant, and the size of the DFZ would change to some other quasi-steady value. Each iteration with a different aerosol concentration in the chamber should require about 1070 seconds (18 minutes).

#4 ice nucleating ability of NaCl aerosol

This experiment is similar to #1 except that the expansions proceed to colder temperatures. NaCl aerosol is not expected to have any strong ice nucleating ability. However, at sufficiently cold temperatures, many cloud

ORIGINAL PAGE IS
OF POOR QUALITY

droplets which form on NaCl aerosol particles will freeze. Thus the cloud which forms will consist of a mixture of supercooled cloud droplets and ice crystals. The water droplets will evaporate as the wall temperature and vapor fields become reestablished in the chamber, but all ice particles will persist since they will ultimately be in equilibrium with the ice-covered walls. Therefore, the concentration of active ice nuclei as a function of final temperature can be ascertained by simply counting the photographed particles which do not evaporate within the experimental time. Fine scale time resolution of the photographic data is not needed since the end products are those of interest. This operational sequence should probably be repeated several times (not consecutively) to evaluate reproducibility. Each operational period (including six different expansions) requires about 2000 seconds (34 minutes).

II.D Dimensions of the SDI Chamber

The time constants of the responses of the thermal and vapor fields at the center of the static diffusion chamber are proportional to the square of the plate separation (Elliott, 1971). Thus a 12cm plate separation in the SDI could provide approximately a factor 16 more experimental time than a 3cm plate separation (ACPL design specification). This could be a significant advantage for an experiment which capitalizes on the transient readjustment period of the chamber, such as after a rapid expansion. Simulations of experiment #1 were performed with the ACPL Simulator to assess the potential benefits in performing the experiments with larger plate separation. The results are summarized in Figures 8a, 8b and 8c which can be compared with Figures 7a, 7b and 7c where the standard 3cm height was used. In the 12cm case, although the temperature changes (Figure 8b), the water cloud in the center region of the chamber is relatively unaffected by the walls for nearly 400 seconds. This is shown by the relative constancy of the traces of liquid water content (Figure 8a) and droplet radius (Figure 8c) at the center and two adjacent grid locations, which together cover a space 1.2cm wide.

The suggestion was made that this would be sufficient time to pursue the original experiment by supporting an ice germ in the SDI with large plate separation. However, such an experiment would not be isothermal, and some additional consideration should be taken of the possible effects of the side walls on experiment #3 since the aspect ratio of the chamber would change from a very favorable 10 (dimension parallel to temperature gradient divided by dimension

ORIGINAL PAGE IS
OF POOR QUALITY

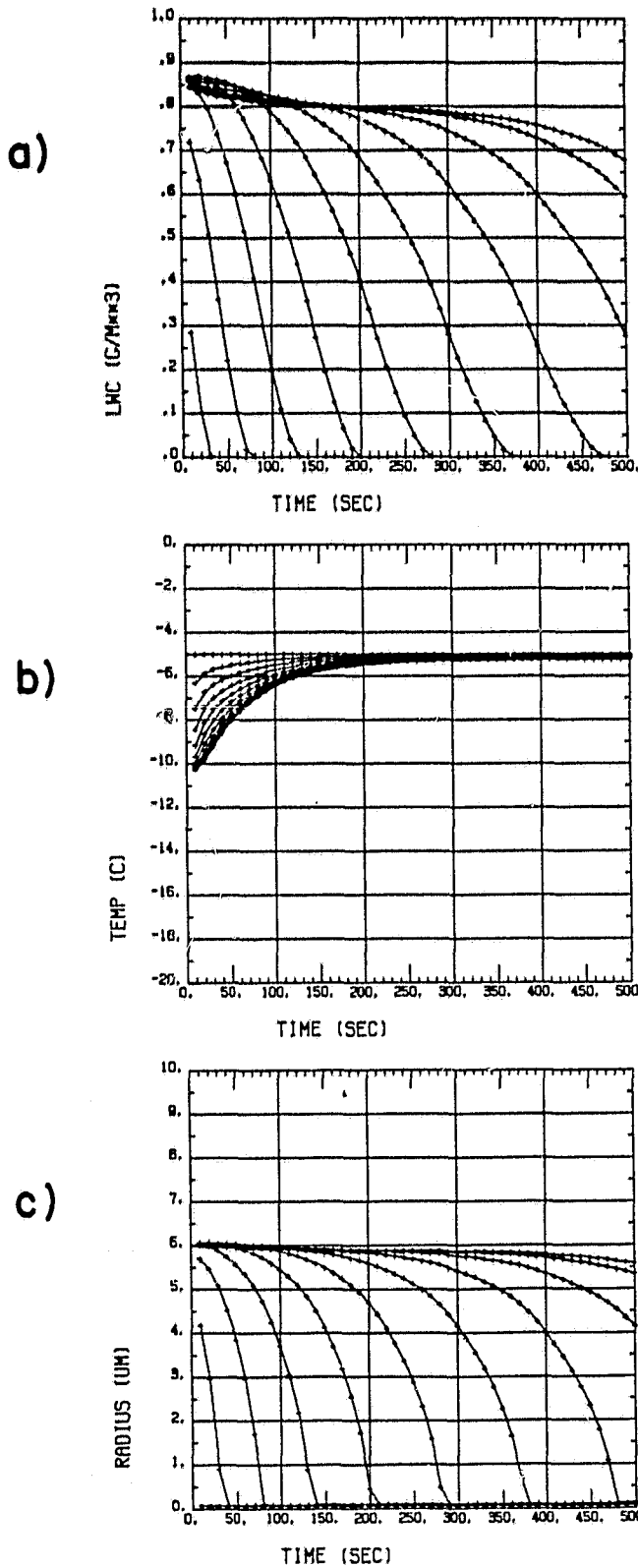


Figure 8a, 8b and 8c. Time traces of temperature, liquid water content and drop radii in a large plate separation SDI as predicted by the ACPL Simulator. With initial conditions of ice saturation at -5°C , a rapid expansion occurs at time zero (-50mb/s for 2 seconds). Values are shown at ten evenly spaced grid locations from the wall to the center. SDI plate spacing is 12cm ; grid spacing is 0.6cm . The experiment is identical to that of Figure 7 except the ice covered plates are further apart; note the change in time scale.

perpendicular to temperature gradient) to a less desirable value of 2.5 (Elliott, 1971, suggests values no smaller than about 6). The other ancillary experiments (#1, 2 and 4) could be performed with some compromise in a 12cm SDI.

III. NUCLEATION OF ICE CRYSTALS IN WINTER OROGRAPHIC CLOUDS

With the reorganization of the ACPL program, we changed our research plans to study the formation of crystals in natural supercooled clouds (our letter of June 20, 1980). There were two aspects of this study:

1. Developing two different techniques for measuring natural ice nuclei (one specifically for deposition and condensation-freezing ice nuclei and another for submicron contact ice nuclei).
2. Analyzing some selected case studies of microphysical data from instrumented research aircraft flights made previously in supercooled cap clouds.

Our major effort for the latter part of this contract was expended on these studies. The results of these studies are briefly summarized in this section. Detailed accounts of the research are in Deshler (1982) and in Rogers (1982).

III.A Measurements of Ice Nuclei with a Continuous Flow Diffusion Chamber

A technique for measuring ice nuclei both below and above water saturation was developed using a continuous flow thermal gradient diffusion chamber. The chamber volume consisted of the 1cm annular space between two concentric cylinders. Significant characteristics of the chamber design included: concentric cylinder geometry, vertical axis alignment and flow, ice covered walls of ebonized copper and optical detection of ice crystals which form and grow on active nuclei. A mathematical model was constructed to simulate the development of the thermal and vapor fields in the chamber and the response of cloud active particles to these fields. The model calculations indicated that ice nuclei would produce crystals of 5 to 10 μm diameter in the 5 to 10 seconds residence time. The predictions of the mathematical model were compared with the ACPL Simulator CFD model for the growth of water droplets at -15°C and water supersaturations (SSw) of +1% and +5%. The comparisons were quite favorable. Characterizing tests with the chamber were performed at both warm ($+15^{\circ}\text{C}$) and cold temperatures with natural air and with artificial aerosols. These tests confirmed the concepts of chamber operation, particle nucleation and growth and optical detection. They also provided the bases for analyzing the data, namely, recognizing the appearance of ice crystals on active nuclei and discriminating these crystals from smaller haze droplets or dry aerosols.

Natural air was sampled in Laramie during winter in air masses similar to those in which orographic clouds form over

Elk Mountain, Wyoming. At -15°C and warmer, the results of the ice nucleus measurements were summarized by two linear equations which gave ice nucleus concentration as functions of ice supersaturation (SSI) for deposition and condensation-freezing nucleation modes. The contributions of deposition ($\text{SSw} < 0\%$) and condensation-freezing ($\text{SSw} > 0\%$) were approximately equal at -15°C and warmer; at colder temperatures, condensation-freezing nucleation became dominant.

Complementary to these laboratory studies, analyses of research aircraft measurements in Elk Mountain cap clouds were performed for three case studies. A summary of five years and 26 clouds was also given and suggested that most ice crystals were forming through primary nucleation processes (no ice multiplication). In spite of the large variability of ice crystal concentration (ICC), there was consistency throughout the five years represented.

Finally, the present measurements of ice nuclei were compared with the cap cloud observations, and it was concluded that the nucleus measurements were comparable with the crystal measurements from -15°C to -20°C . There were more ice nuclei measured at warmer temperatures than the mean observed ICC . The range of nucleus concentrations was comparable with the range of ICC from -10°C to -20°C .

Measurements by others of contact ice nuclei from this region were also shown and were comparable with the ice nucleus measurements from this research and with ICC in the Elk Mountain clouds. Measurements of deposition ice nuclei with the membrane filter technique were approximately a factor 15 smaller than the observed ICC and were also much smaller than measurements of deposition ice nuclei with the continuous flow chamber.

The problem commonly encountered by other researchers, where concentrations of nuclei are much less than crystals, was not in evidence for the cold orographic clouds in winter continental airmasses in this study. The physical composition of natural ice nuclei is not known; they are expected to be of mixed sizes and chemical compositions. There is no basis for expecting a priori that deposition, contact and condensation-freezing nucleation are mutually exclusive processes. In fact, the same aerosol particle may have some activity through each of these modes, with perhaps some preferential activity in one mode: the cap cloud observations suggest that contact nuclei are small aerosols, of the order $.016\mu\text{m}$ diameter; a similar size CCN has a critical SSw of about $+1\%$, and at -15°C , a critical deposition ice embryo would also be about the same size.

Some ideas for future experimental studies with the chamber are offered here:

1. The growth rate of small ice crystals could be studied by varying the total flow with supersaturation fixed.

2. The measured change in particle size could be used to extrapolate to the nucleation point and compare with model predictions.

3. Nucleating behavior of different artificial ice nucleants could be studied for deposition and condensation-freezing modes.

4. Other experiments to separate the size of ice nuclei could be pursued with the chamber. For example, in a manner similar to Twomey's (1972) studies of CCN size, natural aerosol could be sorted by size with Nuclepore filters, and the resulting ice nucleus activity could be related to aerosol size.

5. Another possible study would use a continuous flow CCN chamber attached to the inlet of the ice nucleus chamber to grow active CCN at warm temperatures and separate them by impaction from the non-activated aerosol. Since CCN activity is probably a slowly changing function of temperature, the contribution of condensation-freezing ice nuclei could be deduced by comparing ice nucleus measurements for aerosol containing different fractions of the most active CCN.

6. A more ambitious suggestion is to mount a field study to perform ice nucleus measurements upwind of Elk Mountain and simultaneously to perform aircraft measurements within the cap clouds to assess the expected cause and effect relationship between ice nuclei and ice crystals.

III.B Submicron Contact Ice Nuclei

A simple instrument relying on natural forces to transfer aerosol particles to sampling drops was developed and used to measure atmospheric concentrations of submicron contact ice nuclei. A theoretical description of the scavenging rate of aerosol particles by water drops was developed and checked against other calculations and measurements in the literature. Also a measurement of the scavenging rate using a monodisperse fluorescent dye aerosol and 3 sizes of aerosol particles was conducted for the routine ice nucleus sampling conditions. Theory predicts that the scavenging rate is a strong function of aerosol size. The measurements and the theory were found to agree to within a factor two.

The measurement technique consisted of suspending sample drops in a cooled chamber through which aerosol samples were passed. Observations of the number of drops which froze

during the sampling time were used to calculate contact ice nucleus concentrations. In total, approximately 80, 160 and 55 hours of sampling were conducted at temperatures of -11°C , -15°C and -18°C , respectively. Statistical analysis indicated that the measurements at -15°C and -18°C were significantly above the background (where background was defined by the number of drops which froze as filtered, particle-free air was drawn through the chamber); the -11°C measurements were not above background. The results of the measurements for an assumed aerosol radius of $.01\mu\text{m}$ are 1.0 per liter at -15°C and 2.8 per liter at -18°C .

A survey of ice crystal concentrations in stable wintertime clouds was conducted using aircraft measurements made by the Department of Atmospheric Science at the University of Wyoming. The results of 141 cloud passes were presented and compared with the ice nucleus measurements discussed in this paper and with measurements made by Vali (1974), Cooper (1980), and Huffman (1973). The contact ice nucleus and ice crystal concentrations agreed quite favorably with each other as did the three techniques for measuring contact ice nuclei. The measurements of deposition ice nuclei were lower by an order of magnitude.

The conclusion was reached that submicron atmospheric aerosol particles are active as contact ice nuclei. The concentrations of these nuclei are comparable to ice crystal concentrations in stable wintertime clouds in southeast Wyoming. The size range of ice nuclei consistent with the ice crystal concentrations is $.005\mu\text{m}$ to $.05\mu\text{m}$. These observations are consistent with speculations by Cooper and Vali (1981) on the mode of ice formation in stable orographic clouds. Measurements with an instrument sensitive to larger particles (Vali, 1974) suggested that contact ice nuclei of different size ranges exist in similar concentrations. Hence, atmospheric concentrations of contact ice nuclei may be higher than indicated by a single measurement technique. Submicron contact ice nuclei are important for ice formation in smaller clouds because of the rapidity with which they coagulate with cloud droplets and the limited time of an air parcel in a cloud.

The problem of clarifying the mechanism of contact nucleation has not been addressed in this work. Three theories (Fletcher, 1970; Knight, 1971; and Cooper, 1974) have been proposed to explain contact nucleation. Briefly, the theories suggest that contact nucleation occurs either because of a disequilibrium effect in the interfacial energy at the moment of contact, or because the nucleus carries an ice embryo large enough to nucleate the liquid phase, or because of active sites on the dry particle. All three

theories suggest that contact nuclei will be less active as freezing nuclei, and thus the theories are in agreement with the observed behavior of artificial contact nuclei (Gokhale and Goold, 1968; Fukuta, 1975). Measurements of contact nuclei in natural aerosol samples also confirm this behavior (Vali, 1974; Cooper, 1980).

Beyond this, only Cooper's (1974) theory predicts a relationship between the activity of a nucleus as both a deposition and a contact nucleus. The prediction is that a particle active as a contact nucleus will also act as a deposition nucleus at approximately twice the supercooling. If the deposition measurements (Huffman, 1973) are extrapolated to colder temperatures, a comparison can be made with the contact nucleation measurements made here: for a concentration of 1 ice nucleus per liter, the ratio of supercoolings (deposition to contact) is 1.7. This is in substantial agreement with Cooper's prediction, although these nucleus measurements are widely separated in time and probably sample different size ice nuclei. A more careful comparison could now be made by simultaneous sampling of atmospheric concentrations of deposition and contact nuclei of selected size ranges.

Two instruments sensitive to different sized contact nuclei are now available. Deposition nuclei, which are collected on filters, could be size sorted by one of several techniques. Nuclepore filters could be used to discriminate against sampling the larger size ice nuclei. An electrostatic aerosol classifier (Thermo Systems, Inc.) could be used to extract a monodisperse fraction of aerosol for collection on a filter. Even though the concentration of the monodispersed fraction of the aerosol would be significantly less than ambient concentrations, enough particles for a sample could be collected because of the large volume of air which can be sampled with filters. The third possibility is to use an inertial spectrometer (Prodi, et al., 1979) to size sort the atmospheric aerosol onto filters. Some preliminary results using such a procedure have been reported (Prodi et al., 1980).

Another problem which should not be overlooked is the geographical separation of the ice nucleus and ice crystal concentrations reported here. The impact on ice nucleus concentrations from human activity in a town can not be assessed by the measurements discussed here. Although Vali (1974) reported insignificant difference between measurements taken at Laramie and on Elk Mountain, Wyoming, both Huffman (1973) and Cooper (1980) have reported differences.

An attractive possibility which could contribute to an

understanding of both of these problems is to sample atmospheric aerosols on Elk Mountain for a longer period of time. Contact nucleation measurements using two techniques could be made as well as deposition nucleation measurements. Also an instrument is now available for the measurement of condensation-freezing nuclei (Rogers, 1982). Such measurements would be more representative for comparison with ice crystal concentrations. Also comparisons of the deposition and contact nucleation activity of different sizes of atmospheric nuclei could be used to check the predictions of Cooper's theory for the mechanism of contact nucleation.

IV. PUBLICATIONS AND PAPERS

1981

Rogers, D.C. and M.K. Politovich: Meteorology of the wintertime Elk Mountain cap cloud. Second Conference on Mountain Meteorology, Steamboat Springs, Colorado, American Meteorological Society, Boston, Massachusetts, 371-374.

Rogers, D.C. and Gabor Vali: Observational studies of ice crystal production by mountain surfaces inside winter orographic clouds. Eighth Conference on Inadvertent and Planned Weather Modification, Reno, Nevada, American Meteorological Society, Boston, Massachusetts, 54-55.

1982

Rogers, D.C. and M.K. Politovich: Contribution to CCN Workshop report from University of Wyoming group. J. Rech. Atmos. 15, 203-207.

Deshler, T.L.: Contact ice nucleation by submicron atmospheric aerosols. Ph.D. Dissertation, Department of Physics and Astronomy, University of Wyoming, Laramie, Wyoming, 107pp.

Rogers, D.C.: Field and laboratory studies of ice nucleation in winter orographic clouds. Ph.D. Dissertation, Department of Atmospheric Science, University of Wyoming, Laramie, Wyoming, 161pp.

Deshler, T.L.: Contact ice nucleation by submicron atmospheric aerosols. Conference on Cloud Physics, Chicago.

Rogers, D.C.: Measurements of natural ice nuclei with a continuous flow diffusion chamber. Conference on Cloud Physics, Chicago.

Vali, Gabor, D.C. Rogers and T.L. Deshler: Ice nucleus and ice crystal measurements in cap clouds. Conference on Cloud Physics, Chicago.

V. REFERENCES

- Cooper, W.A., 1974: A possible mechanism for contact nucleation. J. Atmos. Sci. 31, 1832-1837.
- Cooper, W.A., 1980: A method of detecting contact ice nuclei using filter samples. Preprints Int. Conf. Cloud Physics, Clermont- Ferrand, France, 665-668.
- Cooper, W.A. and G. Vali, 1981: The origin of ice in mountain cap clouds. J. Atmos. Sci. 38, 1244-1259.
- Deshler, T.L.: Contact ice nucleation by submicron atmospheric aerosols. Ph.D. Dissertation, Department of Physics and Astronomy, University of Wyoming, Laramie, Wyoming, 107pp.
- Elliott, W.P., 1971: Dimensions of thermal diffusion chambers. J. Atmos. Sci. 28, 810-811.
- Fletcher, N.H., 1970: On contact nucleation. J. Atmos. Sci. 27, 1098-1099.
- Fukuta, N., 1975: A study of the mechanism of contact ice nucleation. J. Atmos. Sci. 32, 1597-1603.
- Gokhale, N.R. and J. Goold, Jr., 1968: Droplet freezing by surface nucleation. J. Appl. Meteor., 7, 870-874.
- Huffman, P.J., 1973: Supersaturation dependence of ice nucleation by deposition for silver iodide and natural aerosols. Ph.D. Dissertation, Department of Physics and Atmospheric Resources, University of Wyoming, Laramie, Wyoming, 125 pp.
- Knight, C.A., 1971: Two subjects in nucleation theory. Int. Conf. Cloud Physics, Canberra, Australia, Amer. Meteor. Soc., Boston, Mass., 31-32.
- Marshall, J.S. and M.P. Langleben, 1954: A theory of snow-crystal habit and growth. J. Meteor. 11, 104-120.
- Mason, B.J., 1971: The Physics of Clouds. Clarendon Press, Oxford, 671pp.
- Prodi, V., C. Melandri, G. Tarroni, T. De Zaiacomo, M. Formignani and D. Hochrainer, 1979: An inertial spectrometer for aerosol particles. J. Aerosol Sci. 10, 411-419.
- Prodi, F., G. Santachiara, V. Prodi, and T. De Zaiacomo, 1980: An experimental technique to study the effect of

size on ice nucleation. J. Appl. Meteor., 19, 1448-1450.

Rogers, D.C., 1982: Field and laboratory studies of ice nucleation in winter orographic clouds. Ph.D. Dissertation, Department of Atmospheric Science, University of Wyoming, Laramie, Wyoming, 161 pp.

Twomey, S., 1972: Measurements of the size of natural cloud nuclei by means of Nuclepore filters. J. Atmos. Sci. 29, 318-321.

Vali, G., 1974: Contact ice nucleation by natural and artificial aerosols. Conf. Cloud Physics, October 21-24, Tucson, Arizona, Amer. Meteor. Soc., Boston, Mass., 34-37.

APPENDIX

Status Report No. 1

205-2 Experiment Requirements Document
205-3 Experiment Specification
205-9 Special Hardware Specification Ice Germ
Generator

DOCUMENT TITLE: Status Report #1

DATA REQUIREMENT NO:

EXPERIMENT TITLE: Ice Forming Experiment

DOCUMENT DATA: November 22, 1978

SUBMITTED TO: NASA, George C. Marshall Space Flight Center

PREPARED BY: Department of Atmospheric Science

Laramie, Wyoming 82071

(307) 766-3245

APPROVED:



Gabor Vali, Principal Investigator

PURPOSE OF THIS REPORT:

The purpose of this report is to describe a set of laboratory experiments which have been conducted in support of the ACPL Ice Forming Experiment design effort.

TOPIC

An important question concerning this experiment is the nature of the profile of cloud droplet density as a function of distance from the growing ice crystal. This is important with respect to the optical recording of that profile and with respect to the data reduction and evaluation processes. From casual observations of similar nature in the past, it was anticipated that the evaporation of cloud droplets will proceed in such a fashion that a zone essentially free of droplets will form around the crystal and that there will be a nearly step-wise change from no drops to full cloud density. It was felt that this problem was of sufficient importance and concern that a preliminary experiment be conducted for its examination.

OBJECTIVE

Examine the sharpness of the boundary which develops as the supercooled water cloud evaporates in the vicinity of ice.

APPROACH

This experiment cannot be performed in three dimensions in the terrestrial environment because of the settling of cloud droplets relative to larger ice elements. Therefore, the preliminary experiment had to be conducted with a two dimensional arrangement. We decided to conduct the experiment on a

cold stage which could support a layer of tiny water droplets and an ice crystal.

PROCEDURE

The temperature controlled cold stage used for the experiment could be held at any constant temperature between 0°C and -20°C . The stability of this stage temperature was better than 0.1°C over the experiment duration of about 5 minutes. The cold stage was covered with a thin foil of aluminum to provide a polished surface for making the observation of cloud droplets easier. A coating of mineral oil insured good thermal contact of the foil to the cold stage. The foil was coated with a silicone varnish to make it hydrophobic.

For these initial experiments, ice of large enough sizes was desired to make some control over the shape of the ice possible. To accomplish this, various shapes were cut out of tissue paper, the tissue was soaked with water and placed on the aluminum foil. Lowering of the stage temperature to approximately -15°C led to freezing of the water in the tissue. The next step was to bring the stage temperature to -10°C , at which temperature all of the subsequent experiments were performed. With the stage at that temperature a uniform coverage of tiny droplets was deposited onto the foil by using a nebulizer. In an auxiliary experiment some of the droplets were captured in toluene and photographed under a microscope yielding their sizes as about 10 to 15 μm in diameter.

Using low angle illumination of the droplet layer, areas free of droplets and those covered by drops could be readily distinguished. Photographs were taken on 35 mm film through a low power microscope.

RESULTS

A droplet free zone began to develop around the ice patches immediately after deposition of the droplet layer. The zone grew in size and its boundary appeared to remain easily discernible to the eye. Four series of photographs are shown on the enclosed figures demonstrating the phenomenon.

Measurements of the sizes of the droplet-free zones have showed a nearly linear increase in size with time for ice patches having straight edges and a gradual decrease in the rate of growth of the width of the droplet-free zone for a circular ice patch. The average rate of growth of the droplet free zone was 0.6 mm per minute in these experiments, but this rate is clearly a function of the density of the droplet layer. This density was held constant for these experiments. The initial rate of growth of the zone, for periods less than 10 sec, could not be established accurately, but appeared to be faster than the subsequent rate of growth.

A total of five experiments were conducted, two with straight edges, one with a circular ice patch, one with a 120° point and one with a 60° point. All experiments yielded the same results, except for the gradual decrease in the rate of growth for the circular patch, which is to be expected for that geometry. The experiment with the 60° point also revealed that there is a tightening of the gradient from ice to water in the vicinity of the tip.

CONCLUSIONS

These experiments provide encouraging support for the feasibility of the planned experiment. Photographic recording of the depleted zone appears to be feasible. Quantitative determination of the gradient from the

depleted to the undepleted region was not possible in these experiments but it appears that the transition is rapid so that details of the transition may not have to be known for the experiment to be meaningful. Further studies will have to be conducted to determine what degree of refinement in that regard will be required.

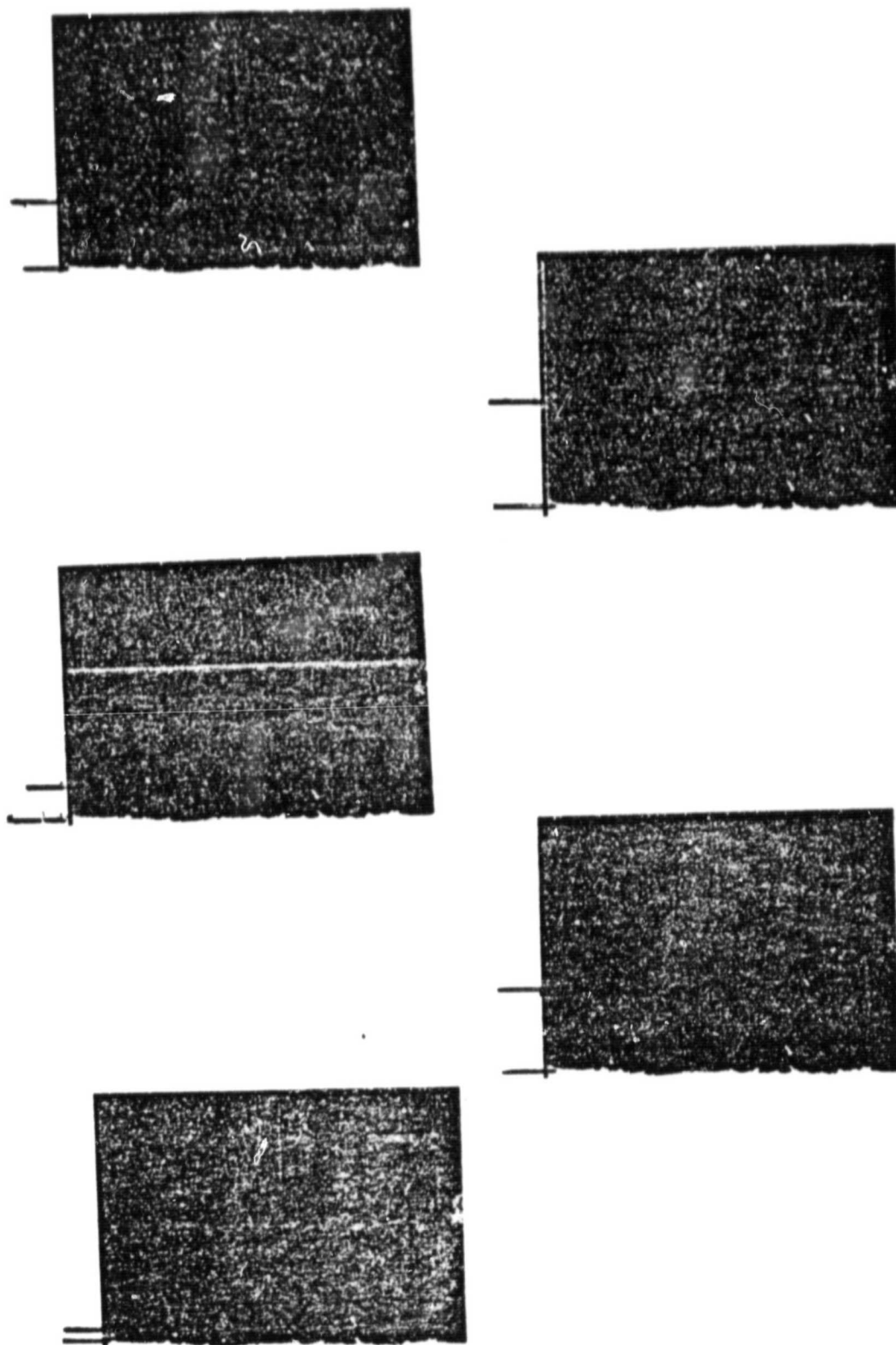


Figure 1. Sequence of five photographs of the growing droplet-free zone next to ice. Width of zone is marked by bars at the top of each frame. Time interval between frames was 30 seconds. Multiplication: 17x

ORIGINAL PAGE
BLACK AND WHITE PHOTOGRAPH

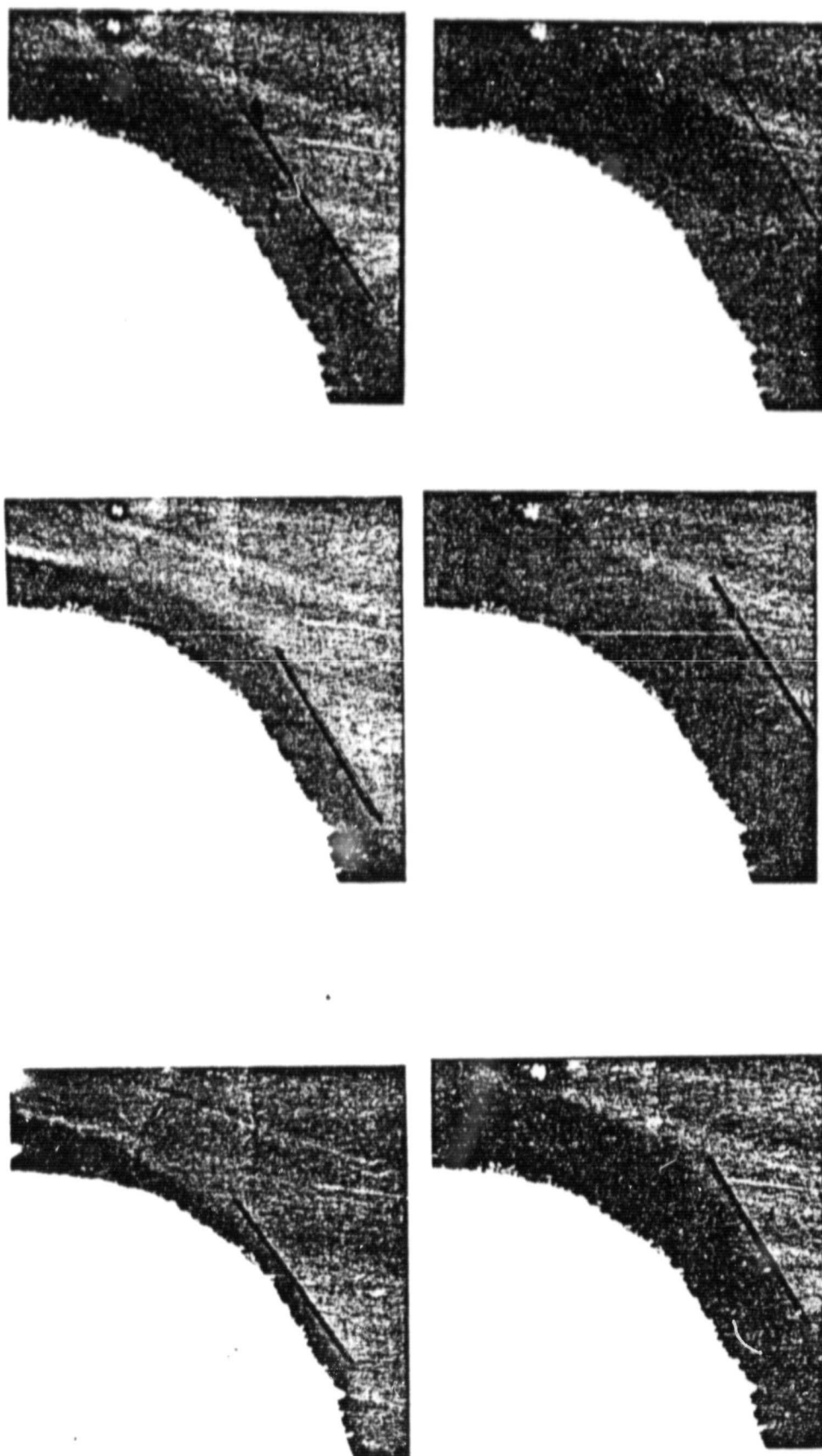


Figure 2. Sequence of five photographs of the growing droplet-free zone next to ice. Width of zone is marked by bars at the top of each frame. Time interval between frames was 30 seconds. Multiplication: 17x

ORIGINAL PAGE
BLACK AND WHITE PHOTOGRAPH

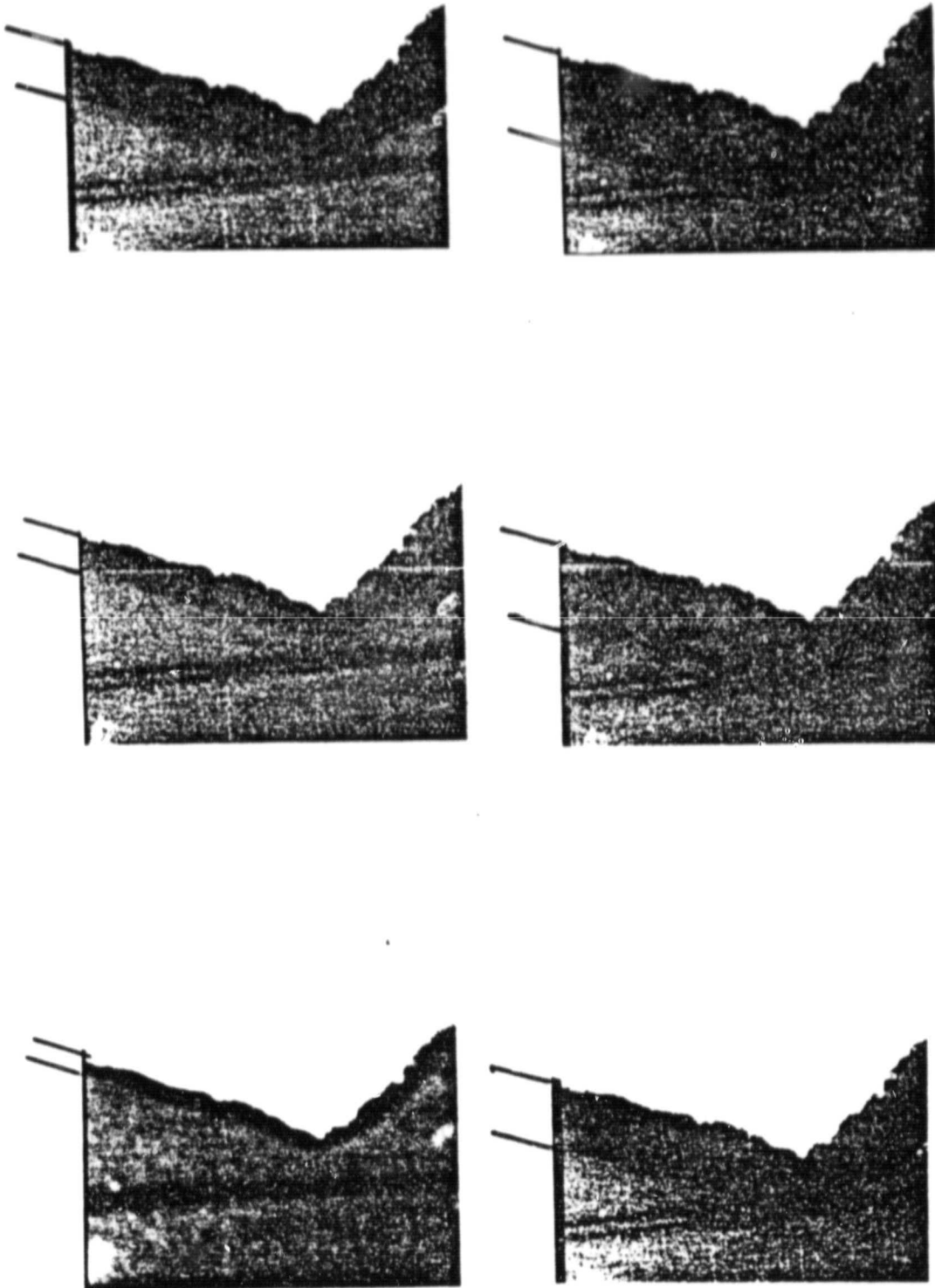


Figure 3. Sequence of five photographs of the growing droplet-free zone next to ice. Width of zone is marked by bars at the top of each frame. Time interval between frames was 30 seconds. Multiplication: 17x

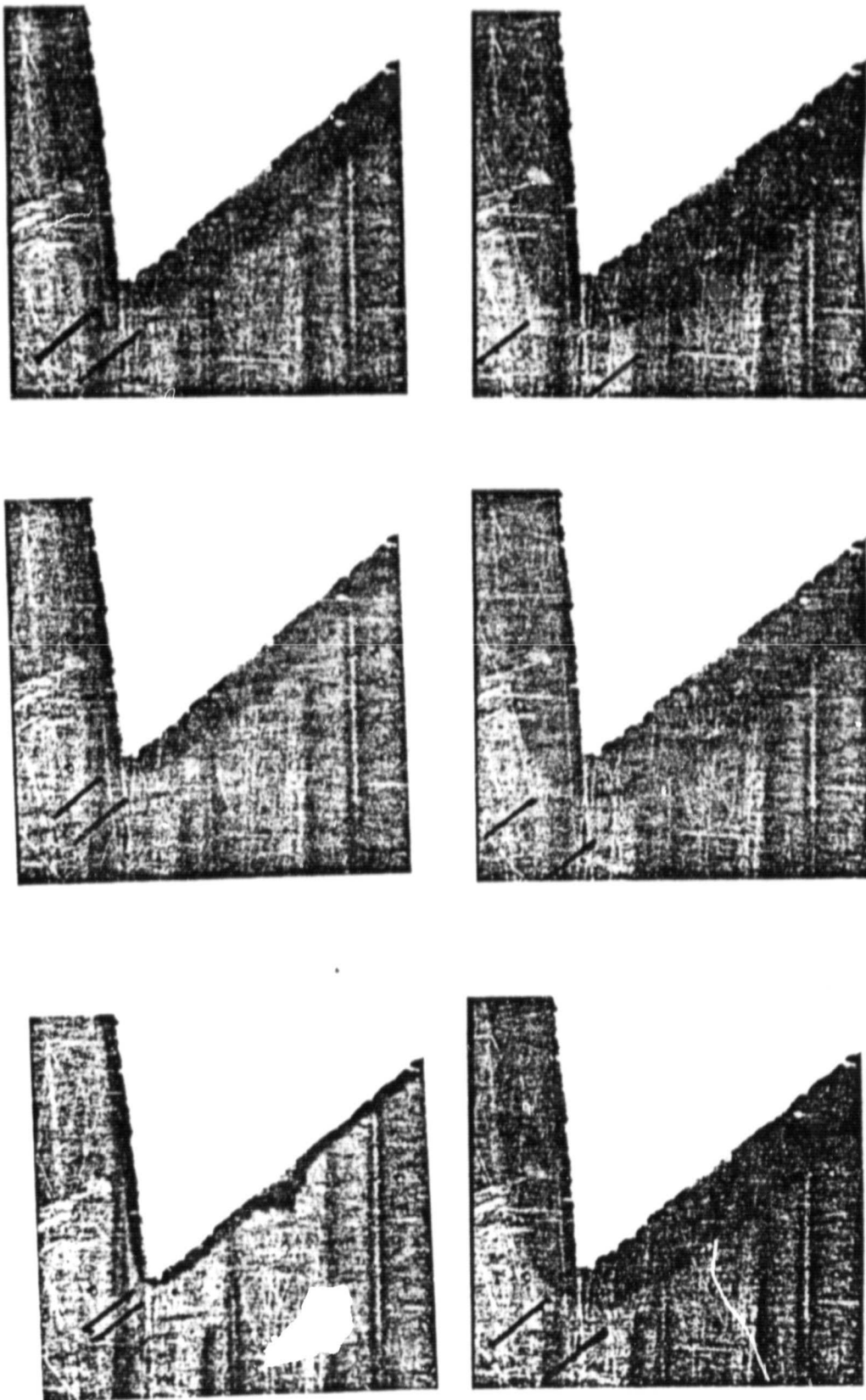


Figure 4. Sequence of five photographs of the growing droplet-free zone next to ice. Width of zone is marked by bars at the top of each frame. Time interval between frames was 30 seconds. Multiplication: 17x

ORIGINAL PAGE IS
OF POOR QUALITY

Rogers

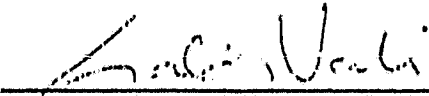
DOCUMENT TITLE: Experiment Requirements Document

DATA REQ'T NO.: 205-2

EXPERIMENT TITLE: Ice Forming Experiment

DOCUMENT DATE: August 7, 1979

PREPARED BY: Department of Atmospheric Science
P.O. Box 3038, University Station
Laramie, Wyoming 82071
(307) 766-3245

APPROVED: 
Gabor Valli, Principal Investigator

ORIGINAL PAGE IS
OF POOR QUALITY

ICE FORMING EXPERIMENT REQUIREMENTS DOCUMENT

RESPONSES TO TABLE I

REQUIRED EXPERIMENT DATA

6 August 1979

1. Experiment Description and Objective

The overall scientific objective of the experiment is to improve the theory of ice crystal growth in clouds, by examining the impact of the normally used simplifying assumption that the presence of cloud droplets around growing crystals can be characterized by saturation vapor pressure over water at an infinite distance from the crystal.

Four different uses of the SDL are planned for ACPL-1 to support the E-Chamber experiment scheduled for ACPL-2 or -3. Requirements for both chambers are given in this document. The essence of the experiments is to ascertain the effect of a liquid water cloud upon the growth rate of an ice crystal.

Using the E-chamber of the ACPL, a supercooled cloud will be created and into that cloud an ice germ will be introduced. The development of a droplet-free zone around the ice germ will be recorded photographically. The evolving size and form of the ice germ will also be recorded on the photographs. This experiment will be repeated with different conditions. From the photographic data the influence of cloud proximity on the crystal growth rate will be evaluated.

2. Experiment Protocol

See Tables 1.A-1.E for experiment timelines.

3. Detail ACPL Requirements

3.1 E-Chamber

Aerosol

Size Range: Mono, 0.03 μm diameter (+ 20%)

Concentration: 200 cm^{-3} and 1000 cm^{-3} (+ 20%)

Type: NaCl

Initial Conditions

Temperature: ranging from 30.0°C to 16.0°C

Relative Humidity: Saturator will be operated at dew point temperatures of 18.0°C to -8.0°C.

ORIGINAL PAGE IS
OF POOR QUALITY

Purge Time: TBD (to fill with characterized aerosol).
Stilling Time: TBD (to reach 0.03 cm s^{-1} velocity)
Expansion: Chamber will be initialized at 1000 mb
and will be operated at final pressures ranging
from 600 mb to 440 mb. Expansion rates TBD.
Photographic: Time period; duration of cycle or TBD
Rate: 2 per sec for first 3 sec, 1
per sec for subsequent 27 sec, 1 per
3 sec for subsequent 70 sec and 1 per
10 sec for remaining time of each cycle
(run).

Visual Observations

Purpose: Confirm proper ice germ generation and camera
focus
Time period: Duration of cycle or TBD
Resulting actions: Immediately inform POCC
Samples: ✓
Gas - not essential
Aerosol - not essential

3.2 SDL Chamber

Aerosol

Size range: Mono, $0.1 \mu\text{m}$ radius ($\pm 20\%$)
Concentration: 1000 cm^{-3} ($\pm 20\%$)
Type: NaCl

Initial Conditions

Mean T: -15°C to -5°C
 ΔT : 0°C
Purge time: 60 - 300 sec, includes generation and charac-
terization of aerosols
Stilling Time: 50 sec or velocity $< 0.01 \text{ cm sec}^{-1}$
Supersaturation levels: $SS_i = 0\%$, $SS_w = -9.3$ to $+3.0\%$
Aitken mode: Yes, initial pressure: 1000 mb
final pressure: ranging from 900 mb
to 655 mb
Photographic: Time period: 60 sec for Experiments #1, #2
and #4 (Tables 1.B, 1.C, and
1.E. 140 sec for Experiment
#3 (Table 1.D)
Rate: 1 per sec for Experiments #1 and #2
1 per 5 sec for Experiment #3
As instructed in Timeline (Table 1.E)
for Experiment #4

Visual observations: Confirm proper ice germ generation as well as camera alignment and focus. Payload Specialist expected to give POCC a complete verbal description of observations through the SDL optical port.

Samples:

Gas - not essential

Aerosol - not essential

3.3 CFD Chamber

Will be used for characterization of the NaCl aerosol for its activation spectrum.

4. Data Requirements

E-Chamber: Initial: T_{s_i} , T_{e_i} , T_i , P_i for $i = 1$ to 15

Rate and Time period: TBD

Photos: 2 per sec for first 3 seconds, 1 per sec for subsequent 27 sec, 1 per 3 sec for subsequent 70 sec, and 1 per 10 sec for remaining time of each cycle (run).

Saturator: T_{s_i} for $i = 1$ to 15

SDL: T_i , T_f , P_i , P_f , SS_w , T .

Photos: 1 per sec, 1 per 5 sec, or as specified - in Timeline in Table 1.//

Housekeeping: TBD

5. Payload Specialist Functions

It will be necessary during these experiments for the P.S. to install the ice germ generator on the SDL or E-Chamber port before the start of the experimental sequence and generate an ice germ manually during each run. The P.S. will also be required to visually confirm proper ice germ generation as well as camera alignment and focus. In the case that adjustable flash illuminated width is needed, the P.S. will make that adjustment prior to each experiment or perhaps during an experiment.

Some of the most useful information available at POCC during the experiment will be the verbal communication with the P.S. and his descriptions of observations through the optical port. He should be trained to a level of competency that he can recognize, interpret, and communicate and cloud physical processes which could occur.

ORIGINAL PAGE 13
OF POOR QUALITY

6. POCC Requirements

Computations: TBD

Communications: Visual descriptions of any ongoing cloud
physical processes within the chambers by
the P.S.

Special Support Hardware: TBD

Software: TBD

7. Spacelab Environment Requirements

Acceleration: acceleration level of up to 10^{-4} g tolerable.

TABLE I.A EXPERIMENT MILESTONE CHART
ICE FORMING EXPERIMENT

ACTION	TIME(S)	COMMENT
1. Insert Ice Germ Generator	0	
2. Set conditions for aerosol density of 1000 cm^{-3}		
3. Start purge of E-chamber with saturator at T_{Si} and chamber at T_{Ei}		Values of T_{Si} , T_{Ei} , T_i , P_i , specified in Table 2
4. Stop purge		
5. Start expansion		Rate of expansion T90 as compromise between speed and stilling time
6. Confirm cloud condensation at P_i , T_i and continue expansion		
7. Stop expansion at T_i , P_i		Time from step 7 to give $v < 0.03 \text{ cm s}^{-1}$
8. Generate ice germ and start photography		P.S. to confirm proper ice germ formation and camera focus
9. Stop photography. Reset ice germ generator. Start heating and dumping E-chamber		
10. to 16. Repeat steps 3 to 9 for second T_{S2} , T_{E2} , T_2 , P_2 .		
17. to 107. Repeat for T_{Si} , T_{Ei} , T_i , P_i to $i = 15$		
108. Change aerosol subsystem to aerosol density of 200 cm^{-3}		
109 to 150. Repeat steps 3 to 9 for $i = 5, 7, 9, 13, 14, 15$		

ORIGINAL PAGE IS
OF POOR QUALITY

TABLE 1.A Continued

27 3.5
267.25
277.55

ICE FORMING EXPERIMENT
E-CHAMBER RUNS

FINAL		LWC	LCL		INITIAL		ORDER
T _i	P _i		T _i	P _i	T _{EI}	T _{SI}	
						Psi 1000mb.	i
- 8	606	1	- 3.3	665	30.0	2.5	13
- 8	606	3	3.8	775	25.5	7.5	10
- 8	606	6	11.8	940	17.0	12.6	5
- 8	530	6	10.5	800	29.3	13.8	4
-8	530	9	17.2	960	20.5	18.0	1
-16	545	1	-10.0	610	30.0	-3.5	14
-16	545	3	-0.6	740	24.7	3.8	11
-16	545	6	9.0	915	16.5	10.5	7
-16	480	6	8.0	800	26.7	11.4	6
-16	480	9	15.0	960	18.5	15.7	2
-24	490	1	-15.0	572	30.0	-8.0	15
-24	490	3	-3.2	70	24.0	1.2	12
-24	490	6	7.3	900	16.0	8.9	9
-24	440	6	6.0	800	24.5	9.0	8
-24	440	9	13.5	960	17.0	14.2	3

$\Delta p = 65 \text{ mb.}$
 $\Delta \rho / \rho = .4 \times 10^{-3} / 1.12$
 $\Delta p = 370 \text{ mb.}$
 $\Delta \rho / \rho = 1 \text{ mb.} / 1.370$

T IN °C, P IN MB, LWC IN GM⁻³

TABLE 1.B Experiment milestone chart
#1 - EVAPORATION OF DROPLETS TO WALLS

ACTION	TIME (sec)	COMMENT
1. Purge SDL, generate and characterize aerosol	0.0	Same as #1
2. Fill SDL with aerosol laden air	300	
3. Standardize pressure and bring walls to initial temperature	400	p = 1000 mb ($\pm 5\%$), SSI = 0%, $\Delta T = 0$, see table below for initial values
4. Stilling time and allow for thermal and vapor equilibrium	550	Same as #1
5. Start photography at frame rate of 1 per sec	600	
6. Rapid expansion to final pressure	601	See table below for final pressures.
7. Stop photography	660	Total of 60 frames
8. Pressurize to 1000 mb	661	
9. Iterate to #3 and use new values for initial and final p and T	670	Refer to table
10. End of sequence	940	Estimated time for two iterations

Experiment #1 - Final pressures, initial wall temperatures, final dry adiabatic temperatures and maximum droplet diameter based on the indicated droplet concentrations: initial pressure 1000 mb.

T_i ($^{\circ}\text{C}$)	-15.0 (± 0.1)	-5.0 (± 0.1)
T_f ($^{\circ}\text{C}$)	-23.0	-13.0
P_f (mb)	900. (± 5 .)	900. (± 5 .)
D (μm)	4.0	5.3
	5.8	7.7
	8.6	11.4
	12.4	16.5
		(3000 cm^{-3})
		(1000 cm^{-3})
		(300 cm^{-3})
		(100 cm^{-3})

ORIGINAL PAGE IS
OF POOR QUALITY

ORIGINAL PAGE IS
OF POOR QUALITY

TABLE 1.C EXPERIMENT MILESTONE CHART

//2 - Ice germ generator and expansion-formed cloud

ACTION	TIME	COMMENT
1. Attach generator to port and seal SDL	0.0	Done by PS
2. Purge SDL, generate and characterize aerosol	60.0	Same as #1
3. Fill SDL with aerosol laden air	360.0	
4. Standardize pressure and bring walls to initial temperature	460.0	Same as #1
5. Stilling time and allow for thermal and vapor equilibrium of walls and chamber and generator probe	610.0	Same as #1
6. Adjust camera focus and manipulate generator controls to produce an ice particle at probe tip or to eject an ice particle	611.0	Done by PS
7. Start photography at frame rate of 1 per second	651.0	
8. Rapid expansion to final pressure	652.0	
9. Stop camera	712.0	Total of 60 frames
10. Pressurize to 1000 mb	713.0	
11. End of test sequence		

ORIGINAL PAGE IS
OF POOR QUALITY

TABLE 1.D EXPERIMENT MILESTONE CHART

#3 - Ice germ generator and thermal gradient formed cloud

ACTION	TIME	COMMENT
1. Attach generator to port and seal SDL	0.	Done by PS
2. Purge SDL, generate and characterize aerosol	60.	Same as #1
3. Fill SDL with aerosol laden air	360.	
4. Standardize pressure and bring walls to initial temperature of -5°C	460.	Same as #1
5. Stilling time and allow for thermal and vapor equilibrium of walls and generator probe	610.	Same as #1
6. Adjust camera focus and manipulate generator controls to produce an ice particle at probe tip or to eject an ice particle	611.	Done by PS
7. Start photography at frame rate of 1 per 5 seconds	670.	
8. Adjust plate ΔT to produce $SS_w = 0.3\%$	671.	See table below
9. Observe DFZ	700.	PS
10. Adjust ΔT for $SS_w = 1.0\%$	730.	
11. Observe DFZ	780.	PS
12. Adjust ΔT for $SS_w = 3.0\%$	770.	
13. Observe DFZ	780.	PS
14. Stop photography	810.	28 frames exposed
15. Adjust central temperature to -15°C	811.	
16. Iterate to step 7.	930.	Repeat steps 7 - 14 for this new temperature
17. End of test sequence	1070.	Total of 56 frames exposed

Experiment #3 - Temperature operating conditions, table of ΔT ($^{\circ}\text{C}$).

SS_w (%)	mean temperature ($^{\circ}\text{C}$)	
	-5	-15
0.3	8.0	12.7
1.0	8.5	13.0
3.0	9.8	13.9

ORIGINAL PAGE IS
OF POOR QUALITY

TABLE 1.E EXPERIMENT MILESTONE CHART

//4 - Ice nucleating ability of NaCl aerosol

<u>ACTION</u>	<u>TIME(S)</u>	<u>COMMENT</u>
1. Purge SDL, generate and characterize aerosol	0.0	aerosol; 0.1 μ m radius, (+10%), 1000/cm ³ (+10%), dew point $\leq -10.0^\circ\text{C}$
2. Fill SDL with aerosol laden air	300	
3. Standardize pressure and bring walls to initial temperature	400	p = 1000 mb (+5%), T = -10.0 (+0.1 $^\circ\text{C}$), SSI = 0%, $\Delta T = 0$, SSW = -9.3%
4. Stilling time and allow for thermal and vapor equilibrium	550	greater of 5 thermal time constants or velocity < 0.01 cm/s
5. Take one photo	600	first of series
6. Rapid expansion to final pressure	601	See Table X below for final pressures
7. Take photo halfway to p_f	602	
8. Take photo at p_f and set frame rate to 1 per 5 sec		
9. Stop camera	661	(present calculations suggest that 60 sec should be enough to allow all water drops to evaporate)
10. Pressurize to 1000 mb	662	
11. Iterate to step //3 and use new values for final press.	670	estimate 270 sec per iteration
12. End of test sequence	2020	total time using all six tabulated values

Experiment //4 - Final pressures, dry adiabatic temperatures and maximum droplet diameters based on initial pressure of 1000 mb, initial temp. of -10°C , and 1000 droplets cm⁻³.

T_f ($^\circ\text{C}$)	-15	-20	-25	-30	-35	-40
p_f (mb)	935	873	814	758	705	655
D (μ m)	5.8	7.2	8.2	9.0	9.7	10.2

ORIGINAL PAGE IS
OF POOR QUALITY

TABLE 1-1 FUNCTIONAL OBJECTIVES

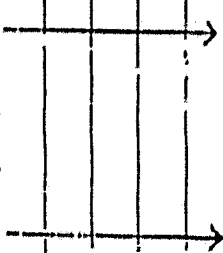
<u>NO.</u>	<u>FO TITLE</u>	<u>OBJECTIVE OR PURPOSE</u>	<u>PI</u>
<u>1</u>	<u>ICE FORMING</u>		
1(a)	Ice Forming Experiment	To evaluate the contribution to crystal growth rate by cloud drops in the crystal's proximity via vapor diffusion in the absence of relative motion between the droplets and the crystal	Vali
1(b)	Evaporation of Droplets to Walls	Document the evaporation of expansion-formed droplets to the isothermal, ice-covered walls; to test the capabilities of the illuminator and camera system; to detect the DFZ boundary; to examine the sharpness of the DFZ; and to compare with current theoretical expectations.	Vali
1(c)	Ice Germ Generator and Expansion formed cloud	Same as 1(b) only with a different procedure of introducing the ice germ into the SEV.	Vali
1(d)	Ice Germ Generator and Thermal Gradient formed cloud	Similar to 1(c) only that droplets are formed by temperature difference between the plates and not by expansion. Examination of the size of the DFZ and sharpness of its boundary.	Vali
1(e)	Ice Nucleating Ability of NaCL aerosol	Test the inherent nucleating ability of the NaCL aerosol in order to assess its possible usefulness for creating free-floating ice crystals; to assess the likelihood and extent of these ice crystals interfering with an experiment which uses a supported crystal.	Vali

TABLE 2 (continued)

FO NO.	FO TITLE	TEST NO.	E-CHAMBER				CFD	SNL		COMMENTS
			T ₀	dT/dt	dP/dt	P		T _m	Aitken	
1)	Ice Forming Exp.	1	20.5	TBD	TBD	530				P ₀ = 1000 mb
		2	18.5	"	"	480				
		3	17.0	"	"	440				
		4	29.3	"	"	530				
		5	17.0	"	"	606				
		6	26.7	"	"	480				
		7	16.5	"	"	545				
		8	24.5	"	"	440				
		9	16.0	"	"	490				
		10	25.5	"	"	606				
		11	24.7	"	"	545				
		12	24.0	"	"	490				
		13	30.0	"	"	606				
		14	30.0	"	"	545				
		15	30.0	"	"	490				
2)	Evap. of Droplets to walls	1		not applicable	not applicable			-19.0	✓	→
		2		not applicable	not applicable			- 9.0	✓	
3)	Ice Germ Generator & Expan. formed cloud	1		not applicable	not applicable			-19.0	✓	→
		2		not applicable	not applicable			- 9.0	✓	
4)	Ice Germ Generator & Thermal Gradient formed cloud	1		not applicable	not applicable			-15.0	✓	→
		2		not applicable	not applicable			-12.7	✓	
		3		not applicable	not applicable			-13.9	✓	
		4		not applicable	not applicable			-13.9	✓	

ORIGINAL PART IS
OF POOR QUALITY

TABLE 2 (continued)

FO NO.	FO TITLE	TEST NO.	C-CHAMBER				CFD	SDL		COMMENTS
			T_0	dT/dt	dP/dt	P		T_m	Aitken	
5)	Ice Nuclea. ability of NaCL aerosol	1		no	applicable			-12.5	/	mono, NaCl, 0.01 m radius, 1000 cm ⁻³ 
		2		no	applicable			-15.0	/	
		3		no	applicable			-17.5	/	
		4		no	applicable			-20.0	/	
		5		no	applicable			-22.5	/	
		6		no	applicable			-25.0	/	
		7								
		8								
		9								
		10								
		11								
		12								
		13								
		14								
		15								
		16								
		17								
		18								
		19								
		20								
		21								
		22								
		23								
		24								

ORIGINAL PAGE IS
OF POOR QUALITY

DRAFT

DOCUMENT TITLE:

EXPERIMENT TITLE

CONTRACT NO:

DOCUMENT DATE:

PREPARED BY:

APPROVED:

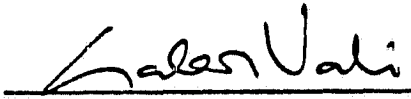
Experiment Specification

Ice Forming Experiment, ACPL-1

NAS8-33150

June 20, 1979

Department of Atmospheric Science
P. O. Box 3038, Univ. Station
University of Wyoming
Laramie, Wyoming 82071
(307) 766-3245



Gabor Vali, Principal Investigator

1.0 SCOPE

This document defines in detail the experiment including objectives, procedures, hardware, and/or subsystem timelines, sample requirements, software requirements, ground facilities, Payload Operation Control Center requirements, data formats, payload specialist requirements, etc. It will include by reference specifications for experiment unique hardware.

2.0 APPLICABLE DOCUMENTS

SVS-9800

205-9 Special Hardware Specification Ice Germ Generator

3.0 EXPERIMENT DESCRIPTION

3.1 General Description

For a general description of the originally proposed experiment, refer to the sequel document (205-3) for the E-chamber. Four different uses of the SDL to support the original experiment are planned; they are outlined here. These uses are closely related to the original experiment in the E-chamber, but they are not a substitute. The essence of the experiments is to ascertain the effect of a liquid water cloud upon the growth rate of an ice crystal.

3.2 Scientific Objectives

For overall objectives, see 205-3. The specific objective of these four ancillary experiments are:

- #1) document the evaporation of expansion-formed droplets to the isothermal, ice-covered walls to test the capabilities of the illuminator and camera system to detect the DFZ boundary, to examine the sharpness of the DFZ and to compare with current theoretical expectations;
- #2) same as #1, but start with an ice crystal in the SEV using the ice germ generator; this is similar to the EC experiment for the brief time that the walls of the SDL do not influence the SEV significantly (about 5 to 10 sec);
- #3) similar to #2, except that the droplets are formed by a temperature difference between the plates and not by expansion; a quasi-steady DFZ should form around the crystal; the points of interest are the size of the DFZ and the sharpness of its boundary;
- #4) test the inherent ice nucleating ability of the NaCl aerosol in order to assess its possible usefulness for creating free-floating ice crystals and to assess the likelihood and extent of these ice crystals interfering with an experiment which uses a supported crystal.

3.3 Mission Plan

Since these experiments are supportive in nature, their main use will be to help define the optimum experimental conditions for the E-chamber experiment. Thus they were designed for ACPL-1 only where no E-chamber is available. Ground research into these and the other experiments will continue, with perhaps greater emphasis upon the ACPL-1 experiments because of the earlier deadlines.

Due to the accelerated time schedule for realigning ACPL-1, the experimental plans outlined here must be viewed as preliminary; they will be brought into sharper focus as the time lag imposed by the schedule realignment is overcome.

3.4 Operation Concepts

Procedures for the four ancillary experiments are briefly summarized in this section. Three will utilize the SDL in a rapid expansion mode: the chamber will initially be isothermal at a temperature below 0°C, and the transient gas temperature will be determined by the amount of expansion. The transient period will last for several thermal time constants of the chamber, and eventually the initial temperature and vapor fields will become re-established. It is the transient period which will be studied by the photographic records during these experiments. The other experiment will use a temperature difference between the plates to form the droplets; the situation is quasi-steady. NaCl aerosol will be used. It will be characterized by the aerosol system for its dry size distribution and by the CFD for its activation spectrum.

#1) Evaporation of droplets to walls

A cloud of supercooled water drops will form during the expansion. Our current simplified calculations suggest that the drops will grow to peak sizes of about 5 to 10 μm diameter. Thereafter, the interior of the chamber will warm by conduction from the walls, and the initial pre-expansion vapor field will become re-established. This will result in the evaporation of all liquid drops within roughly 10 to 20 seconds.

The phenomena of interest are the rate of evaporation of the droplets and the ability of the photographic system to document the evaporation. Adjustments of the initial and final conditions are contemplated in order to push the limits of the photographic system or to enhance the boundary of the drop-free zone. These adjustments, however, tend to work in opposite directions: on the one hand, increasing the aerosol concentration will enhance the contrast along the drop-free zone boundary, but it also reduces the droplet size and therefore taxes the resolution of the photographic system (required to detect 4.0 μm diameter drops). For example, estimated maximum drop diameters using aerosol concentrations of 100 to 3000/cm³ vary from 12 to 4 μm , respectively. Therefore, in order to better examine the capabilities of the photographic system, additional iterations may be desirable, where the aerosol concentration is varied.

The overall time required for each experimental sequence, where expansions at two different initial temperatures are performed, is about 940 sec (16 minutes).

#2) Ice germ generator and expansion-formed cloud

The generator will be inserted into the chamber through a probe port, and the generator will then produce ice on its tip while the payload specialist is controlling and observing its operation. This will be followed by a cloud-producing expansion and photographic recording of the effect of the ice crystal upon the liquid cloud. Since the effects of the walls dominate all processes in the SDL, the time allowed for observing the droplet evaporation is rather limited and is a critical factor for this experiment. It is anticipated that several versions of the ice germ generator will be used: the liquid drop dispenser, the ice ejector and the nucleating substrate fiber. An advantage provided by the zero-g environment is in seeing where an ejected ice particle will go, and if its trajectories are reproducible and controllable for later use in the E-chamber experiment.

#3) Ice germ generator and thermal gradient-formed cloud

The generator will be inserted into the chamber through a probe port, and the chamber will then be cooled to a sub-freezing isothermal condition. The generator will then produce ice on its tip while the payload specialist is controlling and observing its operation. Next, the chamber wall temperatures will be adjusted to produce nominal water supersaturation in the SEV. A water cloud should form in the central region of the chamber except near the ice crystal. The drop-free zone around the crystal will extend from the crystal surface (at ice saturation) outward to where the saturation level increases to water saturation. Since the vapor flux to the ice crystal is much smaller than the flux from the walls, the ice crystal will be a significant vapor sink only over a relatively small region (at least for as long as the crystal remains small). Therefore, the DFZ will be a steady, or quasi-steady, feature; its dimensions will depend upon the crystal temperature, the nominal central supersaturation, the crystal size and the droplet concentration.

This experiment is more difficult to analyze because of two dimensional temperature and vapor gradients, however it has distinct advantages for assessing the sensitivity of the DFZ to the various cloud conditions which are not transients. For example, the central temperature could be changed while keeping the nominal supersaturation constant, and the size of the DFZ would change to some other quasi-steady value. Each iteration with a different aerosol concentration in the chamber should require about 1070 seconds (18 minutes).

#4) Ice nucleating ability of NaCl aerosol

This experiment is similar to #1 except that the expansions proceed to colder temperatures. Thus the cloud which forms will consist of a mixture of supercooled cloud droplets and ice crystals. The water droplets will evaporate as the wall temperature and vapor fields become re-established in the chamber, but all ice particles will persist since

they will be in equilibrium with the ice-covered walls. Therefore, the concentration of active ice nuclei as a function of final temperature can be ascertained by simply counting the photographed particles which do not evaporate within the experimental time. Fine scale time resolution of the photographic data is not needed since the end products are those of interest. This operational sequence should probably be repeated several times (not consecutively) to evaluate reproducibility. Each operational period (including the six different expansions) requires about 2000 sec (34 minutes).

4.0 REQUIREMENTS

General requirements to perform these experiments are less demanding than those contained in SVS-9800, and so we defer to those as defining the critical values. Additionally, however, an access port similar to that for the E-chamber will be required in the SDL in order to attach the ice germ generator. Also, the fine spatial resolution needed to identify the boundary of the drop-free zone may require the adjustment of the flash illuminated width to a value less than 1 cm, or TBD. This problem is still under study, and our progress is summarized in the experimental status report for the period ending May 31, 1979.

4.1 Operational Characteristics

A. Performance

A system which performs according to the requirements of SVS-9800 will be adequate. Preliminary operating values for the experiments are given in the timelines in the next section.

B. Experimental timelines

Preliminary timelines for the four experiments have been prepared using the currently available calculations.

It should be emphasized that the proper choice of operating conditions relies heavily upon simulation support from NASA. These preliminary timelines were prepared in order to try to meet the planning needs of the experimental design, but they are very likely to be modified when more sophisticated simulation support is available.

C. Alternate Experiment Timelines and Methods

TBD

D. Safety

There are no special safety hazards.

E. Physical

Experiment-unique hardware is the Ice Germ Generator, as per 205-9 Special Hardware Specification.

TABLE 1.1 Experiment milestone chart
#1 - EVAPORATION OF DROPLETS TO WALLS

ACTION	TIME (sec)	COMMENT
1. Purge SDL, generate and characterize aerosol	0.0	Same as #1
2. Fill SDL with aerosol laden air	300	
3. Standardize pressure and bring walls to initial temperature	400	p = 1000 mb ($\pm 5\%$), SSI = 0%, $\Delta T = 0$, see table below for initial values
4. Stilling time and allow for thermal and vapor equilibrium	550	Same as #1
5. Start photography at frame rate of 1 per sec	600	
6. Rapid expansion to final pressure	601	See table below for final pressures.
7. Stop photography	660	Total of 60 frames
8. Pressurize to 1000 mb	661	
9. Iterate to #3 and use new values for initial and final p and T	670	Refer to table
10. End of sequence	940	Estimated time for two iterations

Experiment #1 - Final pressures, initial wall temperatures, final dry adiabatic temperatures and maximum droplet diameters based on the indicated droplet concentrations; initial pressure 1000 mb.

T_i ($^{\circ}\text{C}$)	-15.0 (± 0.1)	-5.0 (± 0.1)
T_f ($^{\circ}\text{C}$)	-23.0	-13.0
P_f (mb)	900. (± 5 .)	900. (± 5 .)
D (μm)	4.0 ,	5.3 (3000 cm^{-3})
	5.8	7.7 (1000 cm^{-3})
	8.6	11.4 (300 cm^{-3})
	12.4	16.5 (100 cm^{-3})

TABLE 1.2 EXPERIMENT MILESTONE CHART

#2 - Ice germ generator and expansion-formed cloud

ACTION	TIME	COMMENT
1. Attach generator to port and seal SDL	0.0	Done by PS
2. Purge SDL, generate and characterize aerosol	60.0	Same as #1
3. Fill SDL with aerosol laden air	360.0	
4. Standardize pressure and bring walls to initial temperature	460.0	Same as #1
5. Stilling time and allow for thermal and vapor equilibrium of walls and chamber and generator probe	610.0	Same as #1
6. Adjust camera focus and manipulate generator controls to produce an ice particle at probe tip or to eject an ice particle	611.0	Done by PS
7. Start photography at frame rate of 1 per second	651.0	
8. Rapid expansion to final pressure	652.0	
9. Stop camera	712.0	Total of 60 frames
10. Pressurize to 1000 mb	713.0	
11. End of test sequence		

TABLE 1.3 EXPERIMENT MILESTONE CHART

#3 - Ice germ generator and thermal gradient formed cloud

ACTION	TIME	COMMENT
1. Attach generator to port and seal SDL	0.	Done by PS
2. Purge SDL, generate and characterize aerosol	60.	Same as #1
3. Fill SDL with aerosol laden air	360.	
4. Standardize pressure and bring walls to initial temperature of -5°C	460.	Same as #1
5. Stilling time and allow for thermal and vapor equilibrium of walls and generator probe	610.	Same as #1
6. Adjust camera focus and manipulate generator controls to produce an ice particle at probe tip or to eject an ice particle	611.	Done by PS
7. Start photography at frame rate of 1 per 5 seconds	670.	
8. Adjust plate ΔT to produce $SS_w = 0.3\%$	671.	See table below
9. Observe DFZ	700.	PS
10. Adjust ΔT for $SS_w = 1.0\%$	730.	
11. Observe DFZ	780.	PS
12. Adjust ΔT for $SS_w = 3.0\%$	770.	
13. Observe DFZ	780.	PS
14. Stop photography	810.	28 frames exposed
15. Adjust central temperature to -15°C	811.	
16. Iterate to step 7.	930.	Repeat steps 7 - 14 for this new temperature
17. End of test sequence	1070.	Total of 56 frames exposed

Experiment #3 - Temperature operating conditions, table of ΔT ($^{\circ}\text{C}$).

SS_w (%)	mean temperature ($^{\circ}\text{C}$)	
	-5	-15
0.3	8.0	12.7
1.0	8.5	13.0
3.0	9.8	13.9

TABLE 1.4 EXPERIMENT MILESTONE CHART

#4 - Ice nucleating ability of NaCl aerosol

<u>ACTION</u>	<u>TIME(S)</u>	<u>COMMENT</u>
1. Purge SDL, generate and characterize aerosol	0.0	aerosol; 0.1 μm radius ($\pm 10\%$), 1000/cm ³ ($\pm 10\%$), dew point $< -10.0^\circ\text{C}$
2. Fill SDL with aerosol laden air	300	
3. Standardize pressure and bring walls to initial temperature	400	p = 1000 mb ($\pm 5\%$), T = -10.0 ($\pm 0.1^\circ\text{C}$), SSI = 0%, $\Delta T = 0$, SSw = -9.3%
4. Stilling time and allow for thermal and vapor equilibrium	550	greater of 5 thermal time constants or velocity < 0.01 cm/s
5. Take one photo	600	first of series
6. Rapid expansion to final pressure	601	See Table below for final pressures
7. Take photo halfway to p_f	602	
8. Take photo at p_f and set frame rate to 1 per 5 sec		
9. Stop camera	661	(present calculations suggest that 60 sec should be enough to allow all water drops to evaporate)
10. Pressurize to 1000 mb	662	
11. Iterate to step #3 and use new values for final press.	670	estimate 270 sec per iteration
12. End of test sequence	2020	total time using all six tabulated values

Experiment #4 - Final pressures, dry adiabatic temperatures and maximum droplet diameters based on initial pressure of 1000 mb, initial temp. of -10°C , and 1000 droplets cm⁻³.

T_f ($^\circ\text{C}$)	-15	-20	-25	-30	-35	-40
p_f (mb)	935	873	814	758	705	655
D (μm)	5.8	7.2	8.2	9.0	9.7	10.2

F. Human Performance/Engineering

It will be necessary during these experiments for the P.S. to install the ice germ generator on the SDL port before the start of the experimental sequence and generate an ice germ manually during each run. The P.S. will also be required to visually confirm proper ice generation as well as camera alignment and focus. In the case that adjustable flash illuminated with is needed, the P.S. will make that adjustment prior to each experiment or perhaps during an experiment. He will also have to change film between experiments.

Some of the most useful information available at POCC during the experiment will be the verbal communication with the P.S. and his description of observations through the SDL optical port. He should be trained to a level of competency that he can recognize, interpret and communicate any cloud physical processes which could occur.

G. Government Furnished Property List

None

H. Data Requirements

1. Measurements

As per SVS-9800

2. Photographics

As per SVS-9800. Special attention is required to the problem of properly recording the extent of the droplet-free zone which is surrounded by cloud droplets.

1. Operations

TBD

5.0 VERIFICATION

5.1 ACPL Verification

As per SVS-9800

5.2 Experiment Verification

A. General

Verification of the proper functioning of the ice germ generator is detailed in 205-9.

The capability for photographing droplet-ice zone to be verified in ground experiments; Tests are to be made with prototype illumination and camera system in conjunction with P.I. - developed experimental chamber.

B. Phased Verification Requirements

Follow SVS-9800, performed by hardware manufacturer.

C. Verification Cross-Reference Index

TBD

D. Test Support Requirements

TBD

6.0 INTERFACE REQUIREMENTS

TBD

7.0 EXPERIMENT MANAGEMENT AND IMPLEMENTATION

7.1 Organizational and Management Relationships

As per 205-1 Experiment Development Plan and P.I. contract
NAS8-33150.

7.2 Systems Engineering Requirements

Analyses used to develop this experiment specification are contained in the previous P.I. status reports; these analyses are continuing and will be periodically updated as they converge to their final form.

DRAFT

DOCUMENT TITLE: Special Hardware Specification
Ice Germ Generator

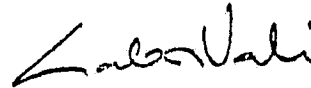
DATA REQ'T NO.: 105-9, 205-9

EXPERIMENT TITLE: Ice Forming Experiment

DOCUMENT DATE: June 1, 1979

PREPARED BY: Department of Atmospheric Science
P. O. Box 3038, University Station
University of Wyoming
Laramie, Wyoming 82071
(307) 766-3245

APPROVED:



Gabor Vali, Principle Investigator

TABLE OF CONTENTS

<u>SECTION</u>	<u>TITLE</u>	<u>PAGE</u>
1.0	SCOPE	1
2.0	APPLICABLE DOCUMENTS	1
3.0	REQUIREMENTS	1
4.0	VERIFICATION	4
5.0	PREPARATION FOR DELIVERY	7

1.0 SCOPE

This specification establishes the requirements of performance, design, and verification of special equipment required for the proposed Ice Forming Experiment selected for the ACPL-1 and ACPL-2 missions. These requirements were not provided by the SVS-9800.

2.0 APPLICABLE DOCUMENTS

SVS-9800

3.0 REQUIREMENTS

3.1 Definition

The following is a description of the Ice Germ Generator required for generating a specified size of an ice crystal in the sensitive experiment volume (SEV) of the Static Diffusion and Expansion chambers as required in the Ice Forming Experiment of the ACPL-1 and ACPL-2 flights.

3.1.1 General Description

The apparatus shall consist of a thin rigid tube, moveable within a sleeve. The tube shall be of minimal diameter yet of sufficient hollowness to allow a liquid drop or ice nucleating substrate of desired size to be extracted and adhered at the tip of the tube. The sleeve shall be constructed for minimal adhesion and shall allow the inner tube to slide back for ejection of the crystal from the end of the tube. The device shall be visible to the cameras and other optics available on the chamber. The apparatus shall be mounted to an accessible port of the chamber allowing for insertion of the generator into the chamber, with the liquid droplet already formed, just prior to performing the ice forming experiment.

3.1.2 Missions

Per SVS-9800

3.1.3 Operational Concepts

Per SVS-9800

3.1.3.1 Ground Operations

A. Installation, Removal, Maintenance
Refurbishment, and Reinstallation

B. Checkout

Per SVS-9800

3.1.3.2 Flight Operations

Per SVS-9800

3.1.4 Organization and Management Requirements

Per SVS-9800

3.1.5 System Engineering Requirements

Per SVS-9800

3.1.6 Critical Components

3.2 Characteristics

3.2.1 Performance

The hardware developed under this specification must meet the following requirements.

3.2.1.1 The tip of the generator shall be located in the center of the SEV and lie in the plane of focus of the recording camera, ± 50 microns.

3.2.1.2 The sleeve shall be of sufficient length such that it shall cover all the inner glass tube, except for the last 5 mm of the tip of generator.

3.2.1.3 The sleeve shall be constructed such that the inner tube can glide easily within the sleeve.

3.2.1.4 The extraction of the liquid droplet before insertion shall be controlled by a pressure valve, such that range of the size of the droplet can be determined to within ± 30 microns diameter.

3.2.1.5 The material of the sleeve shall be constructed to allow minimal adhesion to an ice particle.

3.2.1.6 The tip of the apparatus must be rigid and straight. Vibrations of the glass tip shall be less than 10 micron amplitude during the experiment.

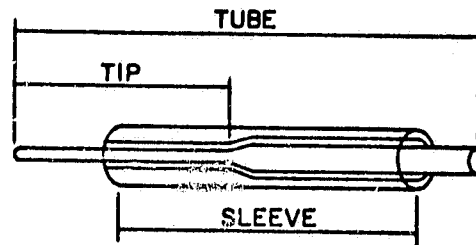
3.2.1.7 The apparatus shall be mounted to the port of the chamber, equipped with a pressure lock assembly allowing for rapid insertion (within 3 seconds) of the generator into the chamber. It shall be capable of cooling and warming without damage. Backup ice germ generating apparatus shall be available.

3.2.1.8 The ice germ generator shall be in a temperature environment greater than 0°C outside the chamber to avoid freezing of the liquid present in the generator.

3.2.1.9 The liquid solution used for the formation of the ice germ shall consist of distilled water and a TBD amount of silver iodide or other TBD ice nucleating substrate. The germ, when inserted into the chamber, shall freeze at temperatures less than -8°C .

May 31, 1979
Page 3

3.2.1.10 The ice germ generating apparatus shall be constructed with the following diagram in mind:



3.2.2 Physical

The inner diameter (ID) of the tip of the glass tube shall be 50 microns and the outer diameter (OD) shall be 100 microns. The expanded portion of the tube shall be 6 cm from the open edge of the glass tip and shall have a 5 mm ID. The hollow sleeve shall have an ID of 200 microns plus the OD of the glass tube, allowing for minimal friction between the inner tube and sleeve. Thus the hollow portion of the sleeve shall be conformed to the contour of the glass tube.

3.2.3 Reliability

Per SVS-9800

3.2.4 Maintainability

Per SVS-9800

3.2.5 Operational Availability

Per SVS-9800

3.2.6 Safety

Per SVS-9800

3.2.7 Environment

Per SVS-9800

3.2.8 Transportation/Transportability

Per SVS-9800

3.2.9 Storage

The ice germ generator shall be stored without potential damage to the tip of the generator.

3.2.9.1 Container

All ice germ generators shall be rigidly stored inside a padded container allowing space for the tip of the tube to avoid contact with any surface.

3.3 DESIGN AND CONSTRUCTION STANDARDS

Per SVS-9800

3.3.1 Materials

Quartz, pyrex glass, or TBD

3.3.2 Contamination Control

Per SVS-9800

3.3.3 Identification and Markings

Per SVS-9800

3.3.4 Workmanship

Per SVS-9800

3.3.5 Human Performance/Human Engineering

Overall design should be such that the operator cannot readily break or degrade the apparatus during insertion, use, and withdrawal.

3.4 LOGISTICS

Per SVS-9800

3.5 PERSONNEL AND TRAINING

Per SVS-9800

3.6 INTERFACE REQUIREMENTS

Per SVS-9800

4.0 VERIFICATION

4.1 GENERAL

Per SVS-9800

4.1.1 Responsibility for Verification

Per SVS-9800

4.1.2 Verification Method Selection

4.1.2.1 Assessment and design techniques shall be employed to minimize the need for testing/retesting.

4.1.2.2 Testing shall be the prime method of requirements verification when any of the following conditions exist:

A. Assessment techniques do not produce conclusive results.

B. Failure mode exists which would compromise personnel safety, adversely affect Shuttle or Spacelab operations, or result in a significant loss of mission objectives.

C. Components are directly associated with inputs to the Spacelab caution and warning system.

4.1.2.3 Verification of Scientific Viability

Rigorous verification of all specifications that have significant impact on the functional capabilities of the equipment and the scientific validity of the data will be required. Principal investigator or alternate will witness verification of scientific viability tests and verify the results of all verification accomplished.

A. Procedure for Verification of Scientific Viability

1. Vibration Characteristics

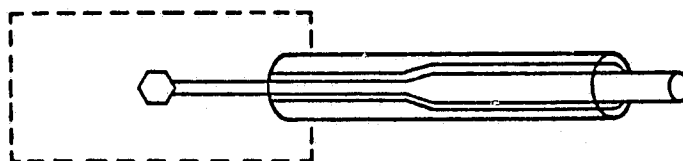
The Static Diffusion Chamber and E-Chamber, with an ice germ generator installed, shall be fitted with instrumentation designed to simulate the acceleration profiles expected aboard ACPL during the flight experiment. Vibration problems shall be assessed by observing any vibration through the use of a microscope. Vibrations of the tip shall not exceed those specified in section 3.2.1.6.

2. Ice Germ Generator Characteristics

Three modes of placing an ice crystal or ice nucleating substrate the SEV will be used in the experiment as denoted in the following figures:

MODE A

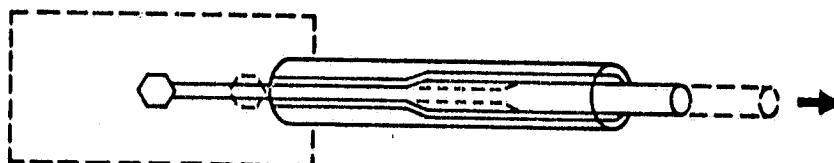
SEV



Sleeve and inner tube remains stationary. Germ remains attached to the tip.

MODE B

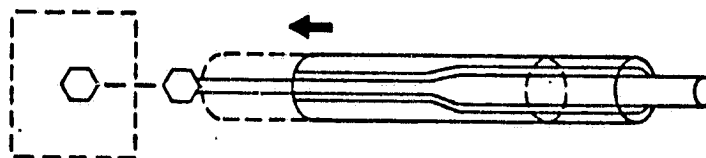
SEV



Inner tube moves back.
Sleeve remains stationary until germ is
dislodged and then sleeve is removed.

MODE C

SEV



Apparatus inserted quickly after cloud formation.
Inner glass remains stationary.
Sleeve moves forward.
Germ ejected from tip to the SEV.

The ice germ generator will be used in each of these modes. Evaluation experiments for tests of each of these modes shall involve the following steps:

a) An ice germ shall be formed (or attached) on the tip of the generator. (The ice germ should also be tested for formation within the chamber).

b) The ice germ generator shall be inserted within the Static Diffusion Chamber or E-Chamber.

c) The chamber shall be cooled to a TBD temperature.

d) The chamber shall be de-pressurized to a TBD pressure allowing for testing of the pressure value for creating the ice germ.

e) The two modes involving ejecting the ice germ from the tip of the apparatus shall be tested during this step.

f) The experiment optics and cameras to be used in flight shall be used to evaluate resolution and quality. Photographs shall be obtained at TBD intervals and TBD magnification.

4.1.3 Relationships to Management Reviews

Per SVS-9800

4.1.4 Test/Equipment Failure

Per SVS-9800

4.1.5 Verification of Unplanned Equipment Uses

4.2 PHASED VERIFICATION REQUIREMENTS

Per SVS-9800

4.3 VERIFICATION CROSS REFERENCE INDEX

Per SVS-9800

4.4 TEST SUPPORT REQUIREMENTS

Per SVS-9800

5.0 PREPARATION FOR DELIVERY

Per SVS-9800